# Fault Detection Algorithms for Spacecraft Monitoring and Environmental Sensing

by

Ashley Kelly Carlton

B.S. Physics
Wake Forest University (2011)



Submitted to the Department of Aeronautics and Astronautics
in partial fulfillment of the requirements for the degree of

Master of Science in Aeronautics and Astronautics

at the

MASSACHUSETTS INSTITUTE OF TECHNOLOGY

June 2016



Author ..... Signature redacted
Department of Aeronautics and Astronautics
May 19, 2016

Certified by ..... Signature redacted
Kerri L. Cahoy
Assistant Professor of Aeronautics and Astronautics
Thesis Supervisor

Accepted by ..... Signature redacted
Paulo C. Lozano
Associate Professor of Aeronautics and Astronautics,
Chair, Graduate Program Committee

# Fault Detection Algorithms for Spacecraft Monitoring and Environmental Sensing

by

Ashley Kelly Carlton

Submitted to the Department of Aeronautics and Astronautics
on May 19, 2016, in partial fulfillment of the
requirements for the degree of
Master of Science in Aeronautics and Astronautics

## Abstract

Constellations of hundreds of low-Earth orbiting small satellites are currently being designed and built. Operators plan to provide data and media distribution services as well as imaging and weather observations. As our society increases its dependence on satellite services for communication and navigation, there is a growing need for efficient spacecraft systems monitoring and space situational awareness to avoid service interruptions due to hazards such as space weather. Particularly for large constellations, satellites need greater autonomy to improve responsivity and reduce the load on human operators.

In this thesis, we present the development of algorithms that identify unusual behavior in satellite health telemetry. Once these events have been identified, we collect and analyze them, along with assessing space weather observations and operational environment factors. Our approach uses transient event detection and change-point event detection techniques, statistically evaluating the telemetry stream compared to a local norm. This approach allows us to apply our algorithms to any spacecraft platform, since there is no reliance on satellite- or component-specific parameters, and it does not require *a priori* knowledge about the data distribution.

We apply these techniques to individual telemetry data streams on geostationary Earth orbit (GEO) communications satellites (ComSats), and consider the results, a compiled list of unusual events for each satellite. Results include being able to identify events that affect many telemetry streams at once, indicative of a spacecraft system-level event. With data from multiple satellites, we can use these methods to better determine whether external factors played a role. We compare event dates to known operational activities and to known space weather events to assess the use of event detection algorithms for spacecraft monitoring and for environmental sensing.

Thesis Supervisor: Kerri L. Cahoy
Title: Assistant Professor of Aeronautics and Astronautics

# Acknowledgments

I would like to first acknowledge and thank my role model and advisor, Kerri Cahoy. Her intelligence, initiative, and compassion both in and out of the classroom serves as an outstanding example to her students. I would also like to thank Jeff Hoffman, Marilyn Good, Beth Marois, my fellow graduate students in the SSL and STAR Lab, and my colleagues at NASA JPL for their continued friendship and guidance.

Lastly, I'd like to thank my family for their relentless encouragement and their sense of perspective. I especially want to thank my partner in life, Matthew Rowen, whose day to day support is in a large part responsible for my success and sanity. Thank you.

# Contents

# List of Figures

# List of Tables

# Key Nomenclature

**ACE** Advanced Composition Explorer

**AU** Astronomical Unit

**CIR** Co-rotating Interaction Region

**CME** Coronal Mass Ejection

**ComSat** Communications Satellite

**EM** electromagnetic

**ESA** European Space Agency

**ESD** electrostatic discharge

**FDD** Fault Detection and Diagnosis

**FDIR** Fault Detection Isolation and Recovery

**GCR** Galactic Cosmic Ray

**GEO** Geostationary Earth Orbit

**GOES** Geostationary Operational Environmental Satellites

**LEO** Low Earth Orbit

**MIT** Massachusetts Institute of Technology

**NESDIS** National Environmental Satellite Data and Information Service

**NOAA** National Oceanic and Atmospheric Administration

**OBC** On-Board Computer

**SAA** South Atlantic Anomaly

**SEM** Space Environment Monitor

**SEP** Solar Energetic Particle

**SEU** Single Event Upset

**SPE** Solar Particle Event

**SSA** Space Situational Awareness

**SSPA** Solid-State Power Amplifier

**SWPC** Space Weather Prediction Center

**SXI** Solar X-ray Imager

**TID** Total Ionizing Dose

**TWTA** Traveling Wave Tube Amplifier

**WDC** World Data Center

# Chapter 1

# Introduction

The near-Earth space environment is hazardous: the ionizing radiation environment and space weather events can lead to component degradation and failures (*e.g.* [9, 40, 77]), and space is becoming more populated, with new constellations of several hundreds of small satellites planned over the next decade to provide communications and navigation services upon which society has become increasingly reliant [127]. This drives a need for spacecraft to be able to quickly identify and react to hazards as well a greater need for situational awareness. In addition, satellites need greater autonomy to improve responsivity and reduce the load on human operators. The goal of this work is to enable remote sensing of space environment, monitoring of system performance, and identification of hazards using telemetry streams. In this thesis, we present the development of algorithms that identify deviations in normal satellite health monitoring telemetry to detect atypical behavior and assess the space environment during events of interest. We use transient detection and change-point detection techniques, which statistically evaluate telemetered values compared to a local norm. The approach does not rely on satellite- or component-specific parameters or knowledge of the underlying data generation distribution, supporting use on any spacecraft platform.

## 1.1 Motivation

Satellites are a growing industry and host critical systems and components that support our society's commercial, scientific, and defense sector infrastructures [52, 90, 110]. For example, satellites provide communications and media distribution, meteorological information, global positioning and timing, reconnaissance, and intelligence services. The reliability of Geostationary Earth Orbit (GEO) Communications Satellites (ComSats) in particular is critical to many industries worldwide, such as for organizations remotely operating offshore oil and gas drilling facilities, where reliable connectivity is key for safety and efficiency [58]. GEO ComSats make up over 50% of the satellties on orbit (with >600 ComSats reported on orbit in 2014), totaling over $203B in revenue in 2014 [110]. The revenue is not in hardware sales, but in the services they provide.

In addition, the increasing demand for and dependence on satellite services has driven technological evolution of spacecraft components to be smaller, more power efficient, and more capable, using smaller feature-size electronics. However, the smaller electronics are more complex and often more susceptible to radiation damage [56].

Given society's reliance on the services satellites provide, satellite failures and other events that degrade performance can disrupt the business of modern life [112, 119]. The harsh space environment, especially the ionizing radiation environment and space weather events, means that almost all satellites will suffer some unexpected or unusual problems – often referred to as "anomalies" – during their lifetime. Anomalies can cause harmful interference or interruptions in service, reduce spacecraft functionality, or cause complete spacecraft failure. Anomalies can be difficult to diagnose and even more difficult to resolve, leading to an increased drain of operator and manufacturer resources (time, money) in both the short and long term [85]. Quick anomaly identification and resolution can mitigate effects of anomalies by reducing interruptions, for example.

### 1.1.1 Space Environment Hazards

The key environments that must be considered when designing and operating spacecraft are: radiation, thermal, vacuum, micrometeoroid, and man-made (radiation and debris). Thermal and vacuum environments can be accounted for the in the design of the spacecraft and tested on the ground, and are fairly well understood near-Earth. The radiation environment presents unique challenges due to the unpredictability of large high-energy (and potentially long duration) events. Therefore, this thesis focuses on ionizing radiation environments and space weather events. Future work includes addressing all aspects of the space environment, particularly motivated by more frequent spacecraft travel beyond near-Earth orbit.

The space radiation environment presents hazards to satellites and the services they provide (internal and surface charging, displacement damage, accumulated dose effects, etc.) causing many documented satellite anomalies (*e.g.,* [9, 40, 44]). As an example, Telstar 401, which was insured for approximately $200M, suffered a complete loss in 1997 following a solar storm [135]. Particles from the Sun in the solar wind and heavy charged particles from galactic sources are a constant bombardment to the environment. Occasional high-energy Solar Particle Events (SPEs) create a mostly unpredictable high-energy particle environment risk. These SPEs heavily influence the location and densities, for example, of the trapped particle radiation environments in Earth's magnetosphere.

The three principal sources of radiation to be considered are those emanating from the Sun, trapped particles in Earth's magnetic field, and galactic cosmic radiation. The Sun produces electromagnetic (EM) radiation, a constant stream of energized plasma called the "solar wind", and solar energetic particles (SEPs) (protons, electrons, heavier nuclei) that are 10s of MeV to GeV. These solar energetic particles are bursty and intermittent, and are part of eruptive events. Explosive conversion of magnetic energy to kinetic and radiative energy produces coronal mass ejections (CMEs) and solar flares, respectively. Solar variability ($\sim$11 year cycle) drives the strength and frequency of SPEs. In the near-Earth environment, energetic particles

are trapped in Earth's magnetic field, called the Van Allen Radiation belts. The belts differ in energy distribution and particle type. While the belts provide protection from the direct effects of solar storms to regions inside the belts, they are a hostile environment to satellites located in or passing through the belts, causing documented satellite anomalies [53]. Galactic cosmic rays (GCRs) are high-energy (up to $10^14$ MeV) particles accelerated to relativistic speeds from events such as supernova explosions. GCRs occur out of phase with the solar cycle and spacecraft are particularly susceptible in orbits crossing the polar regions (where the planetary magnetic field lines are open to space). A more thorough description of the space radiation environments is provided in Appendix A.

Space environment effects on satellites vary according to orbit, spacecraft local time, stage of the 11-year solar cycle, and numerous other factors. Effects can range from simple upsets, which may be easily recovered from, to total mission failure. While reports of anomalies are spread throughout literature, it is often difficult to determine the role of the space environment. The algorithms developed in this thesis will help to determine which of these effects could be responsible for the anomaly or failure.

### Space Environment Effects

The key impacts on satellites due to space weather are: (1) surface charging, (2) internal charging, (3) single event effects (SEEs) or single event upsets (SEUs), and (4) total ionizing dose (TID) effects. Surface charging occurs due to a difference between ambient electron and ion fluxes. Due to their mass difference, electrons are faster than ions, making the ambient electron flux much higher than that of the ambient ions. This leads to differential charging on the surfaces of spacecraft, resulting in possible electrostatic discharges (ESDs). GEO and near-GEO satellites are most at risk due to their movement in and out of the plasmasphere [53]. This can lead to anomalies such as component failures, degradation of sensors and solar panels, and serious physical damage to materials. For example, charging is particularly relevant and dangerous for solar panels, causing a sustained arc, leading to solar array failure on the European

Space Agency (ESA) European Retrievable Carrier (EURECA) satellite in 1993, after only one year of operation [41]. While EURECA operated in LEO, where charging is not usually a concern, EURECA was made of high-strength carbon-fiber struts and titanium nodal points joined together to form a framework of cubic elements. The extended structure made the spacecraft more susceptible to differential charging. See Figure 1-1 for an image of the arcing damage.

Figure 1-1: Damage to the solar array on the ESA EURECA mission due to a sustained arcing event from surface charging. Image Source: Ferguson and Hillard (2003) [41].

Internal (or bulk) charging occurs when high-energy particles (*e.g.,* MeV electrons) penetrate satellite shielding materials and deposit charge on internal spacecraft components. For a typical spacecraft wall with a thickness of 100 mils (2.54 mm) of aluminum, electrons need energies in the range 0.5 - 5 MeV to penetrate, and protons need energies of 10 - 100 MeV (see Figure 1-2 from Garrett and Whittlesey (2012) [48]). If the component's resistivity is high, the rate of charge build up can overcome the leakage rate property of the material. The induced electric field may then exceed the breakdown threshold for the material, causing electrostatic discharges (ESDs) in the material [9, 40, 44, 148]. Lohmeyer et al. (2015) found that the accumulated electric field over the 14 and 21 days leading up to 26 SSPA anomalies on eight GEO

ComSats was high enough to cause the dielectric material in the coaxial cable between the amplifiers to cause breakdown, possibly causing the amplifier failures [78].

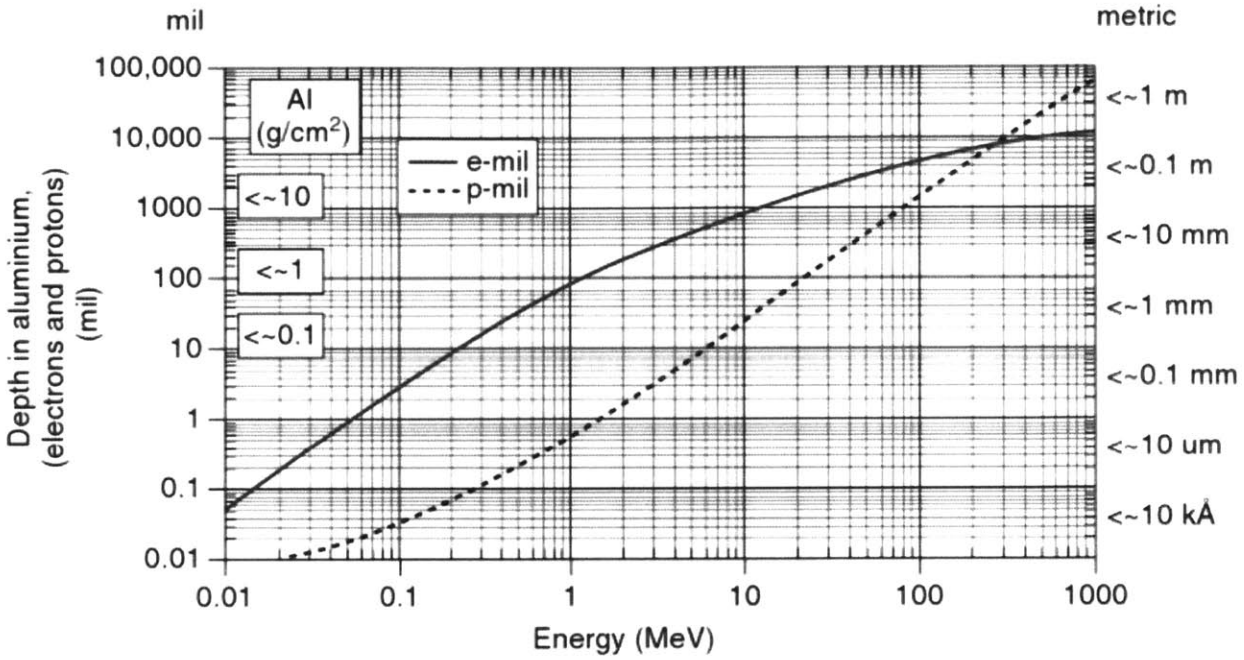


Figure 1-2: Electron (solid) and proton (dashed) penetration depth in aluminum for a range of energies (0.01 to 1000 MeV). For 100 mils (2.54 mm) of aluminum, protons must have energies above roughly 1 MeV and electrons must have energies above roughly 20 MeV. Image source: Garrett and Whittlesey (2012) [48].

Single event effects (SEEs) occur when high-energy particles (>50 MeV), coming from Galactic Cosmic Rays (GCRs) and SPEs, penetrate spacecraft shielding and strikes an electronic device in such as way that the component is affected. Effects can range from simple device tripping to component latch-up or failure. Often, these effects are "bit flips," undesired changes in the logic state of the device. SPEs can also cause increased noise in photonics, total radiation dose problems, power panel damage, and single event upsets [9, 48].

Finally, Total Ionizing Dose (TID) is a result of long-term radiation absorption and can lead to undesirable effects. The total accumulated dose depends on orbit altitude, orientation, and time. The integrated particle energy spectrum (fluence as a function of particle energy) is used to compute the TID. Satellites encounter different annual doses based on the orbit altitude and the thickness of shielding (see Figure 1-3

and Figure 1-4, respectively). As TID increases, material and component degradation increases, leading to reduced functionality and greater susceptibility to failure. There is also evidence that dose rate affects the TID; enhanced effects are seen with lower dose rates ("enhanced low dose rate sensitivity," ELDRS) (see Chen et al. (2010) and references therein [29]).

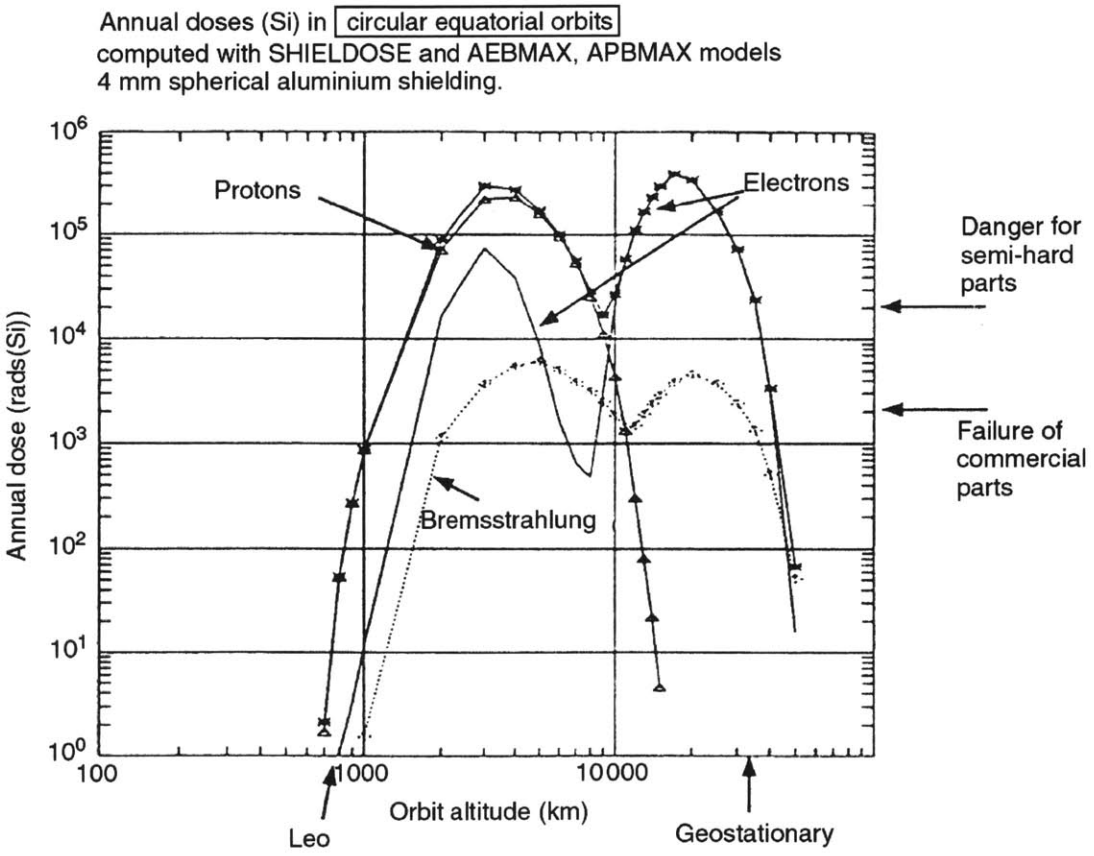


Figure 1-3: Annual dose in rads(Si) as a function of orbital altitude. Contributions are provided from the AE8/AP8 models for protons and electrons through 4 mm spherical aluminum shielding. Image Source: Daly et al. (1996) [32].

We also note that radiation in space may also originate from man-made sources, such as the 1962 Starfish Prime detonation, which generated a temporary artificial radiation belt, crippling or disabling at least six satellites [24, 55].

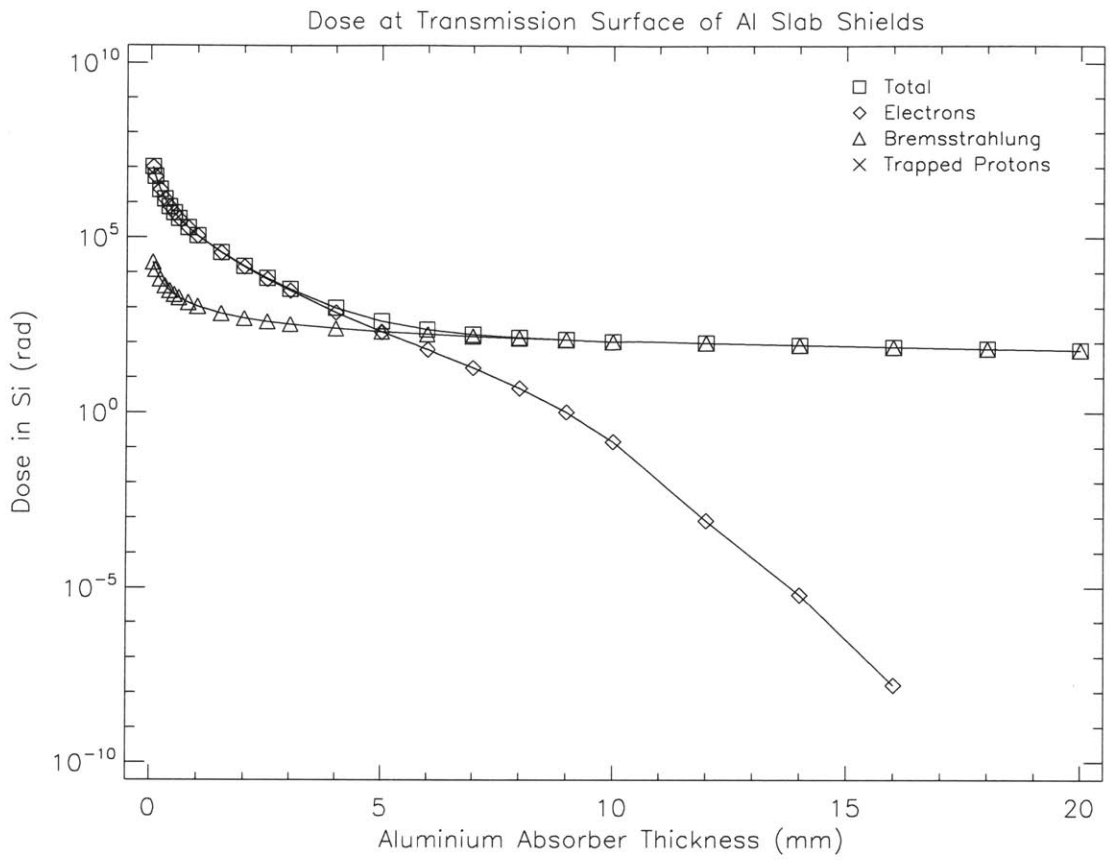


Figure 1-4: Annual dose as a function of aluminum shielding thickness in GEO. This plot was generated using the AE8/AP8 models at solar minimum for the year 2016 for a satellite in geostationary Earth orbit. (For reference, 2.54 mm is equivalent to 100 mils for Aluminum.)

### 1.1.2 Satellite Industry Trends

The near-Earth space environment is becoming more populated, with hundreds of new satellites put in orbit each year. The Satellite Industry Association reports that there are 1261 operational satellites in Earth orbit as of December 31, 2014, totaling $203B in the satellite industry revenue ($322.7B in global space industry), a 4% global growth from 2013 [110]. The population increase means satellites are in closer proximity, leading potentially to increased threats in contested orbits such as in GEO. And, the Low Earth Orbit (LEO) environment is about to become much more populated with the recent push by several industry groups to put large (hundreds) of satellites in LEO (*e.g.,* OneWeb, LeoSat, SpaceX [43]). The increased number of

satellites leads to a need for greater autonomy (operator resources for many hundreds of satellites at once would be enormous), so new operational procedures are necessary.

This ties into the National Aeronautics and Space Administration's (NASA) and others' long term goal of going to Mars and beyond [90, 122]. The longer mission lifetimes mean greater reliability is needed. Communications with the ground will become less frequent (or less timely) as the distance increases, meaning those satellites need greater independence from ground monitoring and interaction. In addition, the environments encountered by the satellites are potentially hazardous, and certainly unknown. Therefore, the ability of a satellite to identify and diagnose anomalies on-board and to be able to identify environmental hazards is growing increasingly important. The ability to infer certain environmental dangers (with minimal impact on already constrained size, weight, and power) allows for faster anomaly resolution and can inform on-board decision-making.

## 1.2 State of the Art

This thesis contributes to three main fields: (1) space environment monitoring, (2) spacecraft fault detection and diagnosis, and (3) space situational awareness. For each of the fields, we have examined the state of the art and the research gap that this thesis addresses.

### 1.2.1 Space Environment Monitoring

One factor contributing to the difficulty of detecting and diagnosing anomalies is the lack of knowledge about the environment local to the spacecraft. It is very challenging to know the root-cause of an anomaly without knowing the space radiation environment experienced by the satellite. While there are several extraordinarily capable spacecraft devoted to space environment monitoring (Geostationary Operational Environmental Satellites (GOES), Advanced Composition Explorer (ACE), Solar and Heliophysics Observatory (SOHO), Van Allen Probes, etc.), these spacecraft are sparsely distributed [92, 96], unable to represent many of the environments

experienced by satellites.

The environment variability is on scales much larger than the current density of space weather monitoring satellites. For example, in GEO, the Geostationary Operational Environmental Satellites spacecraft provide space weather monitoring (in addition to the primary task of Earth observations and monitoring), which the GEO ComSat community relies on for measurements of the environment in the orbit. The current locations of GOES-East (GOES 13) and GOES-West (GOES-15) are 75° West and 135° West longitude, respectively [91]. Coronal mass ejections can range in speeds from 100 km/s to over 3000 km/s. If a GEO ComSat is located at 0° longitude, and the time of day is local noon (*i.e.*, 0° longitude would approximately be the first impact of a Coronal Mass Ejection (CME)), for example, the CME can impact the GEO ComSat over a minute (~109 seconds) before either GOES satellite detects it. For satellites beyond GEO, there is little to no near-real-time information about the local space environment.

Some spacecraft are equipped with radiation detectors, most commonly a dosimeter. Dosimeters measure the TID absorbed by an internal test mass (typically silicon). The device measures the energy absorbed from electrons, protons, and gamma rays, which provides an estimate of the dose absorbed by other electronic devices on the spacecraft.[1] Typical dosimeters are p-FETs or MOSFETs under different amounts of shielding [20].

There is a big effort to move towards smaller radiation detectors to reduce the size, weight, and power (SWaP) demands on the spacecraft. For example, the Teledyne Microelectronics Technologies UDOS001-C microdosimeter, pictured in Figure 1-5, recently flown on the Aerospace Corporation's AeroCube-6 [47], has dimensions of only 1.4" by 1.0" by 0.040" and has a mass of only 20 grams [128].

However, dosimeters are not capable (in general) of discriminating between particle types or their spectra. Different types and energies of particles can have different

[1] A dosimeter does not measure incident energy directly! A dosimeter measures the amount of energy absorbed in a silicon detector due to the energy loss of the particle as it passes through the detector volume. The energy loss is well-characterized in lab tests on the ground for different particles and spectra and through different materials.

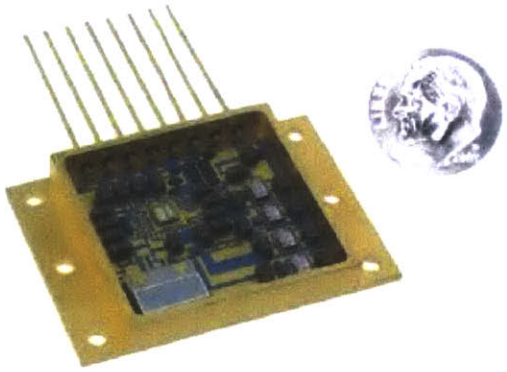

Figure 1-5: Teledyne microdosimter flown on AeroCube-6. Image Source: Teledyne Microelectronic Technologies [128].

effects on spacecraft (*e.g.*, [22, 53]). While efforts have been made to reduce the size, mass, and power of particle-discriminating detectors, state of the art that has flown is still large enough to impact spacecraft design. For example, the ESA Energetic Particle Telescope (EPT) on the Proba-V satellite launched in 2013 is advertised as the smallest particle discriminator to fly and has overall dimensions of 210 mm by 162 mm by 128 mm, with a total mass of 4.6 kg and peak power draw of 6 W [103].

The MIT STAR Lab (in collaboration with the Nuclear Science and Engineering department) is developing a particle spectrometer (called "Sparrow") with the goal of achieving full heavy-ion spectroscopy in a compact, lightweight, and low-cost package. The approach is a scintillator-based pulse shape discrimination, leveraging key innovations in solid plastic scintillators (cheaper, lighter), solid state photomultiplier detectors (replacing large, heavy, photomultiplier tubes for read of scintillation light), and fast analog to digital converters equipped with microcontrollers for digital read-out and processing of analog signals. This device is in preliminary testing, with the goal of an on-orbit flight demonstration in $\sim$2018.

However, just because the local space environment is known does not mean the effects on the individual components or the spacecraft overall are known. This thesis aims to develop algorithms that can detect the local environment on-board the spacecraft directly from monitoring the spacecraft component telemetry. This allows for detection of environments that directly impact components. Dosimeters and particle

spectrometers are designed for detection of specific energies and particle types. Monitoring telemetry allows for detection of hazards that are currently not known (*i.e.*, those for which there are not specific detectors designed). Ideally, on-board detectors could supplement the algorithms, providing validation for events detected in certain instances and assisting with diagnosis.

### 1.2.2 Fault Detection Techniques

Fault Detection and Diagnosis (FDD) techniques for currently operational spacecraft are limited and rely mostly on simple "thresholding" methods at the component-level, and polling schemes at the system-level [87, 136]. Longer mission durations (evolving component performance) and reduced dependence on ground control drive the need for updated FDD techniques.

On the component-level, simple limit checking methods, often called "thresholding" or "out of limits," are used. Numerical limits are set on the upper and lower acceptable values for a particular component. Current thresholding techniques have evolved to include hard and soft limits (for example, failures and warnings, respectively) and thresholds that are applicable for different situations (or operational modes), called "rule-based" methods. However, component performance may change over time, making certain thresholds no longer applicable. This would likely be the case for the SSPA shown in Figure 1-6, where the hypothetical hard thresholds for the first three years of telemetry may have been set at 0.45 and 0.65 for the power amplifier. The performance of the component changed drastically around January 2009, making those hypothetical limits obsolete. In addition, expert knowledge is necessary to decide what the thresholds are for each and every spacecraft component in the first place. The values must be coded specifically for the component.

On the system-level, polling (or voting) schemes are currently used on spacecraft. These methods include "consecutive occurrence counters" and "persistence filters" [87, 129]. They also include rule-based methods, using "if-then" rules encoded by system experts.

Innovative fault detection methods are currently being developed for aerospace

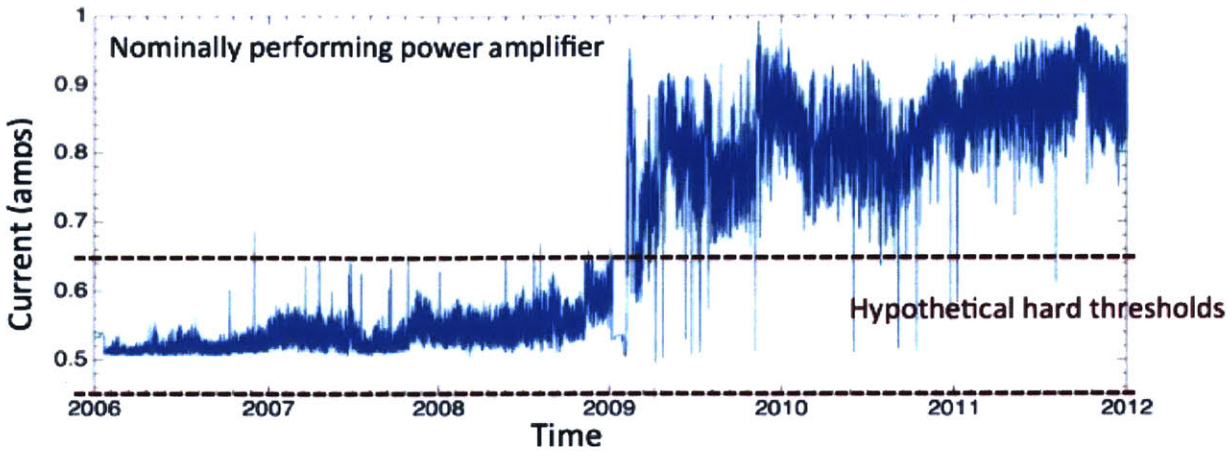


Figure 1-6: Example of the telemetry from a nominally performing power amplifier. The plot demonstrates how changing component performance may render thresholds obsolete after several years on orbit.

applications, but are not yet employed on active spacecraft. Model-based methods, using analytical models, compute residuals between measured and estimated values. There are several aerospace models for this method and current work focuses on developing better dynamical models of systems and components [54, 81]. ESA's SMART-FDIR study in 2003 used the GOCE[2] satellite simulation environment for validation purposes [51]. For detection, no training data was used. Their methods rely on fuzzy inductive reasoning, using a model-based framework. The system behavioral model is decided using possibilistic logic theory, meaning that the behavioral model represents the system knowledge about causal dependencies between inputs and outputs, and are represented by logical formulation. Perhaps the closest to spacecraft flight-ready is the work by Meitinger and Shulte (2009), using a cognitive automation approach, which mimics human cognition (goal-oriented, rational thinkers). Goal directed planning is implemented while considering the current situation. The approach was implemented on a successful UAV flight experiment [83]. However, there are still challenges with this method, since lots of *a priori* knowledge (environment models, models of every subsystem, etc.) is required, increasing the system complexity.

[2]GOCE: Gravity Field and Steady-State Ocean Circulation Explorer, ESA, 2009-2013.

### 1.2.3 Space Situational Awareness

Space situational awareness (SSA) is often just thought of as space surveillance, debris tracking, and conjunction assessment, but the definition includes much more. SSA includes intelligence on the capabilities and intent of unfamiliar spacecraft, space surveillance, reconnaissance, environmental monitoring (including space weather), and satellite command and control.

The Joint Services' definition of Space Situational Awareness (SSA) from Joint Publication 3-14 (2013) states:

> "**[SSA]** is the requisite **current and predictive knowledge of the space environment and the OE[3] upon which space operations depend.** SSA involves characterizing, as completely as necessary, the space capabilities operating within the terrestrial environment and the space domain. SSA is **dependent on** integration space surveillance, collection, and processing; **environmental monitoring, processing and analysis; status of US and cooperative satellite systems;** collection of US and multinational space readiness; and **analysis of the space domain.**"

One of the key functional capabilities the Joint Services describe is Threat Warning and Assessment (TW&A), which involves being about to know the space weather environment, and the ability to predict and differentiate between potential or actual attacks, space weather effects, and space system anomalies, as well as provide timely friendly force status [60].

In ESA's SSA program, the three main areas are (1) surveying and tracking of objects in earth orbit, (2) monitoring space weather, and (3) watching for near Earth objects [38]. As an example of the focus on space weather monitoring, the space weather segment of the ESA SSA Programme took over Proba-2, an observatory with primary instruments for solar monitoring.

Massachusetts Institute of Technology (MIT) Lincoln Laboratory (LL) is actively

[3] operational environment

developing techniques for improvement of SSA. MIT LL agrees with statements that they cannot maintain persistent surveillance on all space catalog objects [1]. They examine non-cooperative GEO monitoring, in which space analysts have no information about the satellite station keeping and maneuvers. The space surveillance data provide the only method to determine orbital status. Detailed in a recent publication called "Decision Support in SSA," MIT LL is using Bayesian networks to combine signature metric information from space surveillance sensors, which allows for MIT LL to detect satellite status changes and produce automated alerts [1].

### 1.2.4 "Spacecraft as a Sensor"

There have been many efforts to use the "spacecraft as a sensor," most notably by the Aerospace Corporation in El Segundo, CA, starting in 1997. Bowman and DeSieno (2012) patented their work on the subject, called "Detecting, Classifying, and Tracking Abnormal Data in a Data Stream". They have developed neural network-based methods (see Section 2.3.4 for a more detailed description of fault detection algorithms). The method is able to adapt to the dataset, but relies on historically labeled training data [23]. Training data instances must be classified as anomalous or nominal. Called "supervised learning," using labeled training data has advantages. It allows for encoding information about basic trends and allowable values.

However, this thesis work aims to detect anomalous events without the use of training data due to the lack of availability or applicability of training data. Often, there is not an identical (or similar) mission for reference training data, making labeled training data nearly impossible to obtain. Operational environments and procedures make the performance degradation unpredictable. The satellite performance and degradation is not well-characterized, meaning that training data from a previous "identical" mission is likely not applicable. Additionally, the labeled training data can prevent the detection of events that have not been "seen" before. However, these methods could supplement this thesis work following a period of time on orbit.

## 1.3 Research Goals and Impacts

Given the harsh space environment, impacting spacecraft performance and lifetime, and projected existence of large constellations, on-board software algorithms must be able to detect anomalies in individual telemetry feeds and intelligently synthesize system-wide data about the performance of its individual parts to provide a spacecraft health state estimation that can help autonomous systems decide what actions, if any, to take [90]. For a fully autonomous system – a system with the ability to act independently of human control (no ground communication) – all on-board decision-making must be derived from spacecraft telemetry and predetermined information stored on-board.

Current fault management strategies, broadly called Fault Detection Isolation and Recovery (FDIR) systems, are typically implemented with both an on-board component and a ground segment [87, 136]. Existing operational strategies for telemetry typically examine only individual streams using what is known as "thresholding," by which the spacecraft On-Board Computer (OBC) may alert operators and/or shut down a component or change operations when that component's telemetry feed shows data that exceeds or drops below pre-defined upper or lower bounds of acceptable values. Although thresholding may detect anomalies, anomaly detection alone cannot ensure prolonged operational capacity. The traditional approach, if certain thresholds are breached, is to "safe mode" the spacecraft, in which all non-essential systems are powered off [129]. However, safe mode is only a viable option when there are systems (or humans) on the ground that are able to identify and resolve the issue(s) leading to the safe mode, and can then command the spacecraft to resume nominal operations.

An autonomous on-board software solution is needed, particularly for large constellations or spacecraft at great distances from their operators. Therefore, efforts to move towards an autonomous on-board software solution are highly desirable [90]. The algorithms must be able to adapt: information about "normal performance" for a spacecraft component may evolve as a mission progresses. For example, the NASA Asteroid Redirect Mission (ARM) has complicated and distinct mission phases in hos-

tile environments, to which OBCs must be aware and adapt [49]. Systems therefore must be able to acclimate to new mission scenarios and events, and they must rely on the information they have (telemetry) to do so. Future extensions of the algorithms developed in this thesis will use machine-learning techniques to evolve the definition of normal performance.

The need to leverage on-board information to learn about the spacecraft health and the environment has led some in the space community to work to develop tools to use the spacecraft itself as a means of detecting potentially hazardous environmental events or potential problems with a system or component. The "spacecraft as a sensor" concept has been explored by the Aerospace Corporation [23] and others (*e.g.,* [45, 59]). The technique these groups have used relies on neural networks. These methods require knowledge of specific components (such as training datasets for neural networks and categories for classification algorithms) or prior knowledge of the system performance (such as the underlying distribution or data patterns). These technologies thus are not designed to adapt to unforeseen events or circumstances. They also are not generalizable to more than the individual spacecraft bus for which they are designed. Unlike current "spacecraft as a sensor" methods, our approach currently does not make assumptions about the underlying distributions and does not impose any component- or satellite-specific parameters or thresholds.

The algorithms can be used on past mission telemetry as well to gather information about the environment, in order to inform future missions. For example, NASA's Juno mission does not carry any space weather detection instruments. However, if environment information can be gathered from the Juno telemetry, valuable knowledge about the Jovian environment can be used for the Europa mission and other future Jovian missions.

The path forward, building upon the algorithms in this thesis, will move the algorithms into real-time operation, incorporating machine learning techniques. This will allow for longer mission durations by providing greater reliability in response to external environment hazards and adaptability to an evolving mission. In addition, the algorithms enable greater sustainability and risk reduction when integrated with

FDIR systems. This thesis presents the approach and results for the algorithms.

In summary, this thesis has **developed algorithms that detect atypical events in spacecraft telemetry, identifying deviations from normal, and avoiding component- or satellite-specific conditioning.** The goal of this work is **to enable remote sensing of space environment, monitoring of system performance, and identification of hazards using telemetry streams.**

## 1.4 Thesis Organization

This thesis is organized as follows: Chapter 1 provides an introduction for the thesis, laying the groundwork and background for the research. Section 1.1 presents the detailed motivation for the study, including the space environment hazards and anomalies due to the environment. Section 1.1 also discusses satellite industry trends towards increased numbers of satellites and longer duration missions. Section 1.2 details the current state of the art for space weather monitoring on satellites (both dedicated and detectors), fault detection techniques, and previous related work by the Aerospace Corporation. Chapter 2 outlines the overall approach to event detection using satellite telemetry. Section 2.3 goes into extensive detail on the characteristics of the telemetry and of the desired detection algorithms, including the challenges that need to be addressed when using a telemetry dataset. We present an overview of fault detection applications and algorithms in other domains. Chapter 3 describes the datasets used for the analysis. The telemetry data are acquired from GEO ComSat operators and the space weather products are provided by National Oceanic and Atmospheric Administration (from the Geostationary Operational Environmental Satellites (GOES) and the Advanced Composition Explorer (ACE)), the World Data Center for Geomagnetism in Kyoto, and the World Data Center in Brussels. Chapter 4 contains the algorithm analyses and results. The transient and change-point detection algorithms are described with examples. The findings are reported for individual telemetry streams, components, and at the spacecraft system level. We highlight findings such as maneuver detection and eclipse entrance/exit. Chapter 4

concludes with a discussion of algorithm sensitivity to tunable parameters and the computational requirements levied by the algorithms. Chapter 5 summarizes the key findings, identifying primary assumptions and vulnerabilities. We conclude with follow-on work for doctoral research and future applications and use cases.

# Chapter 2

# Approach

## 2.1 Overview of Approach

Spacecraft telemetry provides the only source of health information available from a spacecraft, and thus the only indications of a problem.[1] Telemetry, or "measurement at a distance," comes from downlinking electrical signals proportional to the quantity being measured [108, 141]. Spacecraft telemetry originates from sensors and monitors from each subsystem, the payload (if applicable), and from the attitude control system. This work focuses on housekeeping data (sometimes called engineering parameter data or state of health (SOH) data), which is monitored to check the health and operating status of on-board components in subsystems. Housekeeping telemetry can be in the form of an operational or redundancy On/Off statuses, sampled temperature, current, or pressure measurements, or deployment of mechanisms, for example [42]. The telemetry used in this study is from GEO ComSats and is described in further detail in Section 2.2 and Chapter 3. Monitoring each telemetry stream individually provides the "pulse" of a component or of a subsystem.

Relying solely on telemetry, the general approach taken in this work for fault detection for spacecraft health monitoring and environmental sensing is to examine satellite housekeeping telemetry and identify unusual events. Algorithms are used to

[1] Direct observation could show health information, such as loss of control, but direction observation is often not feasible and cannot identify many spacecraft issues, such as loss of communications or power.

identify deviations from what is locally normal in the telemetry. Anomaly detection algorithms have been developed in many domains, such as in finance and medicine. The approach taken in this work uses transient detection and change-point detection techniques, and statistically evaluates the telemetry stream compared to a local norm (see Sections 2.3 and 2.4). This approach allows for application of the algorithms to any spacecraft platform, since there is no reliance on satellite- or component-specific parameters, and it does not require *a priori* knowledge of the data distribution.

For a modern, large communications satellite, there are typically many 1000s of telemetry streams.[2] The algorithms are applied to individual telemetry data streams on a GEO ComSat, and a compiled list of unusual events for each satellite is found. By leveraging a large amount of sensor telemetry, the aggregate dataset, after analysis, enables a spacecraft health state estimation of the entire system, allowing for detection of system-level events and environment-level events. Detected events are compared with known operational activities and with known space weather events to validate the use of event detection algorithms for spacecraft monitoring and for environmental sensing.

## 2.2 Telemetry from GEO ComSat Operators

GEO ComSat telemetry is evaluated in this analysis for two primary reasons: ComSats provide critical services, requiring high reliability that can be helped by fault detection algorithms and an understanding of hazardous space environments, and ComSats have many decades of telemetry, providing a long baseline to evaluate and a large quantity of data.

GEO ComSats make up over 50% of the satellites currently in Earth orbit (38% commercial communications, 14% government communications) with greater than 600 satellites as of December 31, 2014 [110]. While the annual revenue of these satellites totals over $203B [110] and the average communications satellite costs $250M on average to build, launch, and insure [127], the fundamental value is in the services

[2]Personal communications with Intelsat operators (August 2014).

these satellites provide. GEO satellite observations are used to actively monitor terrestrial and space weather, agricultural development, natural hazards (such as wildfire growth), and geological evolution. GEO ComSats also provide communication globally (including to remote locations), reconnaissance and intelligence communications, and emergency response services, making the satellites a critical asset to defense agencies [145]. Interruptions to these services (or failures in these systems) could significantly impact society [94].

ComSats are mature technology with over a half of century of heritage. The first communications satellite was Echo 1 in 1960, and the first GEO ComSat was Syncom 3 in 1964 by Hughes.[3] The design lifetime for a modern ComSat is 10 to 15 years, with many satellites operated beyond this nominal lifetime for return on investment reasons, with increasing interest and development in technologies to extend satellite lifetime [14]. The long mission durations of the satellites, which span the temporal variations in the space environment (mostly importantly, the 11-year solar cycle), and thousands of housekeeping telemetry streams provide a long baseline of telemetry. In addition, operators, such as Intelsat and Inmarsat, operate tens of ComSats simultaneously, adding to the already large dataset. However, the massive amounts of telemetry generated are typically archived by operators and only analyzed in the event of an unexplained issue. Partnering with GEO ComSat operators who maintain these telemetry archives allows for scientific and statistical assessment of events, trends, and relationships to known space and operational environments.

## 2.3 Developing Algorithms to Detect Unusual Behavior and Events

Telemetry is a time-series dataset, where data is obtained from observations collected sequentially over time. The term "event" is used this thesis to describe atypical or unusual behavior or anomalies in the telemetry. "Anomaly" will be used interchangeably with the term "event," though an anomaly is a type of event. Anomalous events

[3]The "Syncom" (synchronous communications satellite) program was started by NASA in 1961.

could correspond to critical and unwanted component performance, leading to the need for anomaly detection techniques. Event detection, in the context of this thesis, also includes novelty detection, which aims to detect previously unobserved events or trends in the data [79, 80]. Anomaly detection for time-series data is a commonly explored domain with many survey studies, such as "Anomaly Detection: A Survey" by V. Chandola et al. (2009), "Mining Time Series Data" by C. Ratanamahatana et al. (2005), and "Time Series Data Mining" by P. Esling and C. Agon (2012). Interested readers may find more detailed information and references in [27, 37, 104].

This section focuses on characteristics of the GEO ComSat telemetry dataset, a summary of the desired algorithm traits, and relevant techniques developed for anomaly and feature detection in other domains. A discussion of the advantages, disadvantages, and assumptions is provided for the selected techniques.

### 2.3.1 Telemetry and Algorithm Characteristics

**Characteristics of Telemetry Dataset** The telemetry dataset is *sequential data*, meaning that the data instances are related to each other and are linearly-ordered (e.g., *time-series* data), real-valued variables. The data are *univariate*: each telemetry stream is a measurement of one sensor or component (only one attribute). For example, a telemetry stream is a sequential set of current measurements from a high-powered amplifier.

**Types of Anomalies** The types of anomalies that can appear in time-series data are point anomalies and contextual anomalies. Point anomalies are when individual data instances can be considered anomalous with respect to the rest of the data. This is the most mature and well-explored area of anomaly detection. Thresholding techniques can often suffice for point anomaly detection. Point anomalies for sequence data, where data instances are related, can often appear as a set, or as collective anomalies [125, 139], constituting a more difficult detection problem.

Contextual anomalies occur if a data instance is only anomalous in a certain context, but perhaps not otherwise. In time-series data, 'time' is a contextual at-

tribute that is used to determine the context (or neighborhood) for that data instance [109, 140]. Context is important because component performance may change over time, due to damage or degradation. As another example, a satellite temperature measurement of 50 degrees Celsius may be allowable during certain times of the mission, but may be contextually anomalous during eclipse periods, when the spacecraft is not directly irradiated by the sun. However, applying a context is not always simple, making it challenging to develop and use such techniques.

**Data Labels: Level of Supervision** Labeled training data (dataset where data instances are labeled normal or anomalous) is difficult or impossible to obtain. In the case of satellite telemetry, every mission is unique. Even if a satellite is designed and built as part of a fleet of identical satellites from one manufacturer, the operational demands and spacecraft environment will be different, making labeled training data inaccurate or non-existent. Therefore, event detection for the dataset of interest is necessarily unsupervised, meaning that techniques do not require training data. Techniques in this category make the implicit assumption that normal data instances are far more frequent than anomalous ones; if this assumption is not true, then the technique may suffer from a high false alarm rate [27].

Anomaly detection for spacecraft telemetry could be, in part, *semisupervised.* Semisupervised techniques assume the training data has labeled instances only for the normal class. Semisupervised techniques could be used after a period of spacecraft operation, building up the training database and a model for the class corresponding to normal behavior, and the model could then be used to identify anomalies in the new data [45].

**Output of Detection Algorithms** The desired output of an anomaly detection technique for telemetry is an 'event score,' indicative of the degree to which a data instance is anomalous. Scoring allows for a list of ranked anomalies. The user can choose to select the top detection(s) or use a cutoff threshold to select the anomalies. Thus, scoring allows for domain-specific thresholds to select the most relevant anomalies.

Scoring can include preferential weighting, given expert knowledge about the system. For example, for space environment monitoring, certain telemetry streams may be more sensitive to the radiation environment, so their anomaly scores may be given a larger weight than those that are less sensitive.

**Algorithm Complexity** Due to the size of the dataset (discussed in more detail in Chapter 3), the computational complexity (time, on-board storage, and processing capability) of the detection algorithms is a key consideration. Complexity of the algorithms will greatly affect whether online (or near real-time) adaptive and dynamic algorithms can be used, or if the events will be detected retrospectively in batch algorithms [37]. For online applications, algorithms that are termed *autocannibalistic* [72], meaning the algorithm is able to dynamically delete parts of itself to make room for new data, offer mitigations to the on-board storage constraints. With regards to processing capabilities, Bhargava et al. (2003) have shown that sending measurements to a central processor is likely energy inefficient and lacks scalability for high volume data streams [16]. Algorithms employed at the component- or subsystem-level may provide a computational savings.

**Summary of Key Desired Algorithm Traits** Given the aforementioned telemetry characteristics in this section and the algorithm requirements described in Section 1.2, the key algorithm traits can be summarized. The algorithm must be able to detect anomalous data instances. The algorithm must also be able to detect contextually anomalous data points, and therefore must be adaptive to a changing notion of normal in time. The algorithms must not (and can not) rely on training or labeled data, as none exists in most spacecraft applications. The algorithm must have a scoring technique that produces a measure of "how anomalous" an event is in the context. This allows for ranking of events. Lastly, the algorithm should not levy heavy computational requirements (time, on-board storage, and processing capability) on the spacecraft system.

### 2.3.2 Challenges in Time-Series Anomaly Detection

There are many challenges associated with time-series anomaly detection. Most notably, defining a "normal" region or time period in the series that encompasses all "normal" behavior is difficult. The boundary between normal and anomalous is often not well-defined. As mentioned in Section 1.2, normal behavior can evolve, *i.e.* a current notion of normal behavior might not be sufficiently representative in the future. And, current anomalous behavior may be normal in the future, leading for the need to detect contextual anomalies in time-series. As will be described in Section 2.3.4, many algorithms operate supervised or semi-supervised. However, the availability of labeled data for training (and for algorithm validation) of models used by anomaly detection techniques is a major issue. Lastly, noise in the data is often difficult to identify and distinguish and to remove from the signal.

A key challenge is that it is difficult to apply techniques in one domain to another; the exact notion of an anomaly is often different in different application domains. Due to the multitude of challenges in anomaly detection, most existing anomaly techniques solve a specific formulation of the problem [27].

### 2.3.3 Fault Detection Algorithms in Other Domains: Applications

Fault and anomaly detection is prevalent in many domains, such as in public health, manufacturing, and finance. Applications of anomaly detection that are similar or relevant to the spacecraft telemetry event detection problem include intrusion detection, fraud detection, medical and public health anomaly detection, and sensor networks [27]. The following sections give a brief overview of the applications listed and the existing detection techniques and challenges.

**Intrusion Detection** Intrusion detection in a system (typically a computer system) refers to detection of malicious activity, such as break-ins and other forms of abuse [100]. A key challenge, which is echoed in telemetry event detection, is the large

volume of data. The data are usually streaming (and sequential), and may require online analysis. Therefore, techniques must be computationally efficient. While the false alarm rate for a technique may be low, the sheer size of the data will magnify the false alarms, which may be a consideration given the time and financial burden of a reaction by spacecraft operators to an alarm. For intrusion detection, in contrast to spacecraft anomaly detection, labeled data for normal is usually available, so semi-supervised techniques can be used (in addition to unsupervised techniques).

Techniques for host-based intrusion detection systems[4] rely on detection of anomalous subsequences (collection anomalies) of the traces (system calls). While all traces belong to the same alphabet, it is the co-occurrence of events that is the key factor in differentiating between normal and anomalous behavior [27]. Techniques are based on subsequence matching and ordering: model the sequence data, or compute the similarity between sequences. The four types of algorithms that are commonly used are statistical profiling using histograms, mixture of models, neural networks, support vector machines, and rule-based systems. Section 2.3.4 compares relevant fault detection techniques, including a brief description of each technique.

Techniques for intrusion detection could be used in the spacecraft telemetry event detection if specific patterns are associated with certain events or anomalies. For example, if a component failure is always preempted with a hyperbolic uptick in the telemetry, followed by a slow decline, these patterns could be identified and reported using models and rule-based systems. However, a model of the normal behavior must be known. In addition, these techniques do not address point anomalies.

**Fraud Detection** Fraud detection generally refers to criminal activities occurring in commercial organizations such as in banks, credit card companies, cell phone companies, the stock market, etc. *Activity monitoring* is the general approach to fraud detection, where the usage profile of a customer is maintained, for example, and the profiles are monitored for any deviations [39]. This application is analogous to monitoring component profiles in spacecraft telemetry, examining for any deviations.

[4]Intrusion detection is typically divided into "Host-Based" and "Network" systems [33].

Applications in credit card and insurance fraud are typically done by comparing individuals to their own usage ("by-owner"), or compared to a profile they fall in ("by-operation"). Contextual anomalies can then be detected by the user as the context for "by-owner," or often the geographic location as the context for "by-operation." Techniques in this field are typically supervised, or semi-supervised, relying on labeled normal data, making them unsuitable for the context of this thesis. Techniques include neural networks, rule-based systems, and clustering.

**Medical and Public Health Anomaly Detection** In the time-series domain, the medical and public health community is interested in anomaly detection in health monitoring sensor outputs, such as electrocardiograms (ECGs) and electroencephalograms (EEGs) [30]. Most techniques are aimed at point anomaly detection and rely on labeled training data from healthy patients, adopting a semi-supervised approach. The key examples are parametric statistical modeling, neural networks, Bayesian networks, rule-based systems, and nearest neighbor based techniques. Collective anomaly detection techniques have also been applied [74].

**Industrial Damage** The industrial damage domain is segmented into two parts for detection: defects in mechanical components (system health management) and defects in the physical structures. For detecting defects in components, the data in this domain is typically temporal, so time-series algorithms have been applied [12, 63, 64]. The anomalies occur mostly because of an observation in a specific context (contextual anomalies) or as an anomalous sequence of observations (collective anomalies). Normally, a semi-supervised approach is used because components without defects are readily available, though unsupervised techniques are also used for unexpected component performance and degradation. Anomalies are often required to be detected in real-time as preventive measures are often required to be taken as soon as the anomaly occurs. Techniques include parametric statistical modeling, non-parametric statistical modeling, neural networks, spectral, and rule-based systems.

For detecting defects in physical structures, the data collected also has a temporal

aspect. Since the application is typically for a structure, the models learned are static over time. The techniques are similar to novelty or change-point detection, and include statistical profiling using histograms, parametric statistical modeling, mixture of models, and neural networks.

**Sensor Networks** The sensor network application is an interesting challenge because anomaly detection can either mean that one or more sensors are faulty, or then are detecting events (such as intrusion). Algorithms detect sensor faults, or intrusions, or both. This application is analogous to the collective spacecraft telemetry system. An anomalous telemetry stream could be from the sensor (*e.g.,* a pressure gauge) rather than the component (*e.g.,* propellant tank). Or, the event detected could be from both the sensor and the component.

Another challenge with sensor networks (that is also present in telemetry networks) is sensor noise: algorithms need to be able to distinguish between interesting anomalies and unwanted noise and/or missing values. This is particularly relevant in spacecraft telemetry (if algorithms are run on the ground) because of the long and complicated transmission path from the satellite to the ground. Discussed in Section 1.2, "online" anomaly detection is desired in order to identify and react to hazards in real-time. For these reasons, anomaly detection methods that consider the entire spacecraft network must be lightweight. Techniques considered in the sensor network domain are Bayesian networks, rule-based systems, parametric statistical modeling, nearest neighbor-based, and spectral techniques.

### 2.3.4 Fault Detection Algorithms in Other Domains: Techniques

The following section highlights common techniques for anomaly detection in time-series data and for the applications mentioned in Section 2.3.3. The discussion is limited to contexts that may apply or be useful to the spacecraft telemetry domain, with its associated characteristics (discussed in Section 2.3.1). Readers interested in general time-series anomaly detection are directed to surveys, such as "Time-Series

Data Mining" by Esling and Argon (2012), for more detailed information [37].

**Classification-based Anomaly Detection Techniques** In classification-based anomaly detection techniques, such as neural networks, Bayesian networks, support vector machines (SVMs), and rule-based, classification is used to learn a model (classifier) from a set of data instances (training) and then classify a set of test instances into one of the classes using the learned model (testing) [34, 126]. The different techniques in the classification-based set differ in their approach to learning the model from the data. In most cases, the algorithms are designed for semi-supervised or supervised learning for learning the model of the data, making this class of algorithms unsuitable for this thesis. In addition, while the testing phase can be fast, the computational complexity of learning the initial model can often be constraining. For example, SVMs involve quadratic optimization. In addition, the results of the techniques generally are the assignment of a label to each data instance, not giving a meaningful anomaly score. Some techniques that obtain a probabilistic prediction score from the output of a classifier (*i.e.,* rule-based), can be used to partly address the scoring issue [101].

For unsupervised learning with anomaly scoring, rule-based classification techniques are the most viable and use association rule mining for one-class anomaly detection [5]. The rules that capture normal behavior are learned using algorithms such as the Ripper rule or decision trees [69, 88]. If the test instance is not covered by any rule, it is considered anomalous. Support thresholds can be used to prune out rules with low support. Each rule has an associated confidence value that is proportional to the ratio between the number of training instances correctly classified by the rule and the total number of training instances. The confidence value can then be used to assign an anomaly score: the inverse of the confidence associated with the best rule is the anomaly score for a given test instance. In addition, training of decision trees is typically fast [62], making rule-based techniques a possible choice for spacecraft telemetry event detection. The key drawback is that these techniques are for one-class anomaly detection, meaning the instances can only have one label.

**Nearest Neighbor-based Anomaly Detection Techniques** The basic assumption for nearest neighbor techniques is that normal data instances occur in dense neighborhoods, while anomalies occur far from their closest neighbors. While anomaly scoring is generally simple (the data instance's distance, often Euclidean, to $k$th nearest neighbor or the relative density of each instance), the challenge with these types of techniques is that the performance is highly dependent on the choice of distance or similarity measure. This technique can operate unsupervised, but if data has normal instances that do not have enough close neighbors, or if data has anomalies with enough close neighbors, the technique fails to label the instances correctly. This, coupled with the performance challenges and the computational complexity ($O(N^2)$), makes the nearest neighbor-based techniques undesirable for spacecraft telemetry event detection.

**Clustering-based Anomaly Detection Techniques** Clustering-based techniques are used to group similar data instances into clusters. The typical scoring metric is the data instance's distance from the closest cluster centroid (cluster-based local outlier factor (CBLOF), for example). While similar to nearest neighbor techniques, clustering-based techniques evaluate each data instance with respect to the cluster to which it belongs (nearest-neighbor techniques analyze each instance with respect to its local neighborhood). The basic technique relies on a clustering algorithm to cluster the data, and then the distance to closest centroid is computed [117]. Thresholds can be set on distance or density of clusters to declare anomalous data instances. A key challenge is the computational complexity (typically quadratic) and high performance dependency on the effectiveness of the clustering algorithms. Effectiveness can be improved through semi-supervised clustering [13]. Clustering algorithms are not optimized to find anomalies, and there are also issues if anomalies form clusters themselves.

**Statistical Anomaly Detection Techniques** Statistical Anomaly Detection Techniques have been used for many decades and, like classification techniques, have a

wide range of applications and variants of algorithms. The underlying principle of any statistical anomaly detection technique is: "An anomaly is an observation which is suspected of being partially or wholly irrelevant because it is not generated by the stochastic model assumed" [8]. The key assumption is that normal data instances occur in high probability regions of a stochastic model, while anomalies occur in the low probability regions of the stochastic model. In general, statistical techniques fit a statistical model (usually for normal behavior) to the given data and then apply a statistical inference test to determine if an unseen instance belongs to this model or not. Instances with low probability are declared anomalous. There are two categories of statistical techniques: parametric and nonparametric, both of which are good candidates for use on spacecraft telemetry event identification.

Parametric techniques make the assumption that the normal data are generated by a parametric distribution. There are three main types of parametric techniques: Gaussian-model based, regression model-based, and mixture of parametric distributions-based. Gaussian model-based techniques are most commonly used and the most heavily explored, including simple outlier detection (*e.g.,* >3 sigma from distribution mean [116]), Box Plot Rule, Grubb's Test, Student's T-Test, and Chi-Squared Statistics. The parameters are known or are estimated using Maximum Likelihood Estimates (MLEs), for example. The anomaly score is the inverse probability density function or the test statistic from a statistical hypothesis test. While the performance is dependent on the choice of test statistic, the computational complexity is typically linear in data size. Regression model-based techniques have a regression model fitted to the data, and then, for each test instance, the residual for the test instance is used to determine the anomaly score. These are popular techniques when training data is available, but caution must be taken, as the presence of anomalies in training data can influence the regression parameters, reducing the accuracy of the results. Robust regression approaches have been developed to mitigate anomaly-induced inaccuracies in the model generation, such as in the commonly used Autoregressive Integrated Moving Average (ARIMA) models [17, 28]. These techniques have been explored in detail for time-series data by Abraham and Box (1979)

and Abraham and Chaung (1989) [2, 3]. For mixtures of parametric distributions-based techniques, there are two subcategories based on the modeling method: model instances and anomalies as separate parametric distributions, or model only the normal instances as a mixture of parametric distributions.

Nonparametric techniques do not assume knowledge of the underlying distribution. The model structure is not defined *a priori*, but is instead determined from the data, typically making fewer assumptions about the data, such as smoothness of density, when compared to parametric techniques. Histogram-based (or frequency- or counting-based) techniques are the simplest and most common. A histogram is used to maintain a profile of the normal data. These techniques are popular in the intrusion detection community [33, 35, 36] and fraud detection [39], since the behavior of the data is governed by certain profiles (user or system) that can be efficiently captured using the histogram model. For the univariate case, there are two basic steps: building a histogram based on the different values taken by the feature (either in the training data or data to date), and then each test instance is checked to see if it falls in one of the bins of the histogram. The performance is impacted by the choice of bin size: if the bins are small, there could be a high false alarm rate. If bins are large, there could be a high false-positive rate. In general, the complexity is linear. Kernel function-based techniques involve using kernel functions to approximate the density (Parzen windows estimation [98], for example). This type of technique is similar to parametric methods, but a density estimation technique is used. The computational complexity (quadratic in terms of data size) is the key issue with kernel-based techniques.

If the assumptions about the underlying distribution hold true, the statistical techniques provide a powerful and capable tool for detecting anomalies, providing a statistically justifiable solution for anomaly detection. A key strength of the statistical techniques is that the anomaly score is provided by the statistical technique, offering a meaningful anomaly score. The score is associated with a confidence interval, which can be used as additional information while making a decision regarding any test instance. The challenge is choosing the best statistic for the hypothesis testing, as it

is often not straightforward. But, the computational complexity is linear, in general. For these reasons, statistical techniques are chosen as the basis for the spacecraft detection algorithms. Nonparametric techniques are explored. And, even though the distribution is unknown, if the distribution estimation step is robust to anomalies in data, parametric statistical techniques can operate in an unsupervised setting without any need for labeled training data, and so are also considered.

**Information Theoretic Anomaly Detection Techniques** Information theoretic techniques analyze the information content of a data set using different measures, relying on the assumption that anomalies in data induce irregularities in the information content of the data set. The techniques can operate unsupervised and do not rely on knowledge of an underlying distribution. Computational complexity is a challenge (often exponential), though approximations of the techniques allow for linear computational complexity. However, it is difficult to associate an anomaly score with a test instance, and the performance is highly dependent on the choice of information theoretic measure. For these reasons, information theoretic techniques are not a good choice for spacecraft telemetry event detection.

**Spectral Anomaly Detection Techniques** Spectral techniques try to find an approximation of the data using a combination of attributes that capture the bulk of the variability in the data [27]. The idea is that the data can be embedded into lower dimensional subspaces in which normal instances and anomalies appear significantly different. The basic technique involves determining subspaces (embeddings, projections) in which the anomalous instances can be easily identified. Principal Component Analysis (PCA) is the basis for several of the techniques, which projects the data into a lower dimensional subspace [61, 97]. Scoring is based on the data instance's distance from the principal components, performed in the same way as the statistical techniques, but in a smaller subspace. However, the computational complexity is often quadratic. In addition, spectral techniques are only useful if the normal and anomalous data instances are separable in the lower dimensional embedding of the

data.

## 2.4 Approach to Identifying Unusual Events for the Spacecraft System

**Component-level** Unusual events in spacecraft system are identified in an incremental approach, increasing the number of telemetry streams considered at each phase. First, the detection algorithms are applied to each individual telemetry stream, identifying events in single telemetry streams. This allows for identification of events at the component-level and component-level monitoring. Then, the events detected from all telemetry streams of a certain type or subsystem are examined, such as all of the thermistors on-board, or all of the components in the propulsion system. Similar performance might be expected from components of the same type, or in the same sub-system, so directly comparing and compiling the events from that component type may yield an event that affects the subsystem-level.

**System-level** The next level of abstraction is at the system-level: the detection of events from the telemetry streams for many subsystems (or the entire spacecraft system) are considered. The intersection of the events may be indicative of an external (environmental) or internal (spacecraft-level) event, having an effect on the spacecraft system. This step allows for system-level monitoring and anomaly detection. A block diagram of system-level detection is given in Figure 2-1. Event scoring from different components or different systems must be considered, however, since some components are likely more sensitive to certain environments or system-level events than others. On the positive side, this event scoring also allows for expert domain knowledge to be included through special weighting of event scores.

**Environment-level** For datasets containing many satellites, the intersection of system-level events from multiple satellites provides the opportunity to detect environmental events (natural or man-made space environment events that could affect a

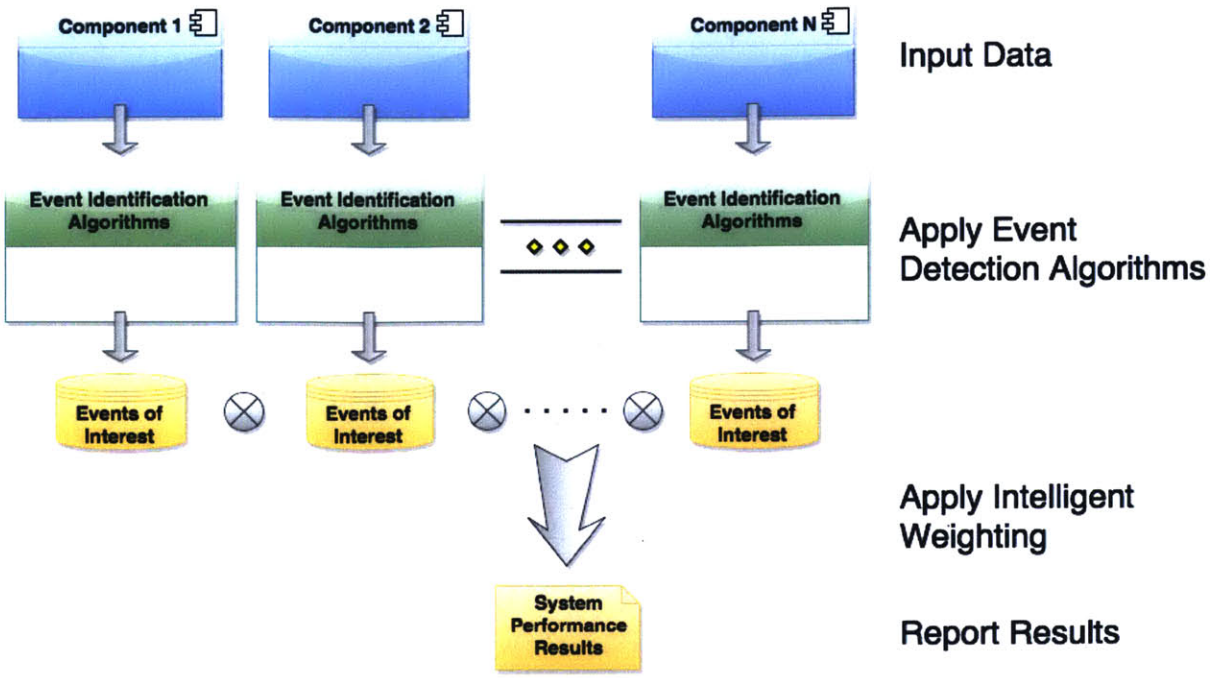


Figure 2-1: Approach for telemetry event detection algorithms applied on system-level.

local environment). The detection of environmental events depends on the location of the satellites and the spatial and temporal frequency of the environmental events to be detected.

# Chapter 3

# Data

## 3.1 Data Acquired

### 3.1.1 GEO ComSat Telemetry

The GEO ComSat telemetry used in this thesis is from MIT partnerships with two commercial operators: Intelsat and Inmarsat, two of the world's leading providers of global telecommunications. Both organizations operate tens of GEO ComSats and have been operating their fleets of GEO ComSats for several decades. Intelsat and Inmarsat are leading the way for scientific research using telemetry by allowing MIT to have access to the data. They also provide invaluable guidance for data interpretation. A summary of the acquired telemetry can be found in Table 3.1.

#### Intelsat

In 2014, we partnered with Intelsat, a D.C.-based telecommunications company, operating with decades of experience, starting in 1965 [58]. We have analyzed over 20 years of archived telemetry from 22 satellites from four fleets (different manufacturers). We acquired current and temperature telemetry from Solid-State Power Amplifiers (SSPAs) and Traveling Wave Tube Amplifiers (TWTAs), solar panel current, total bus power, and shunt loads, and magnetometer measurements, totaling over 0.5 TB of data. We also have Single Event Upset (SEU) lists from four satellites.

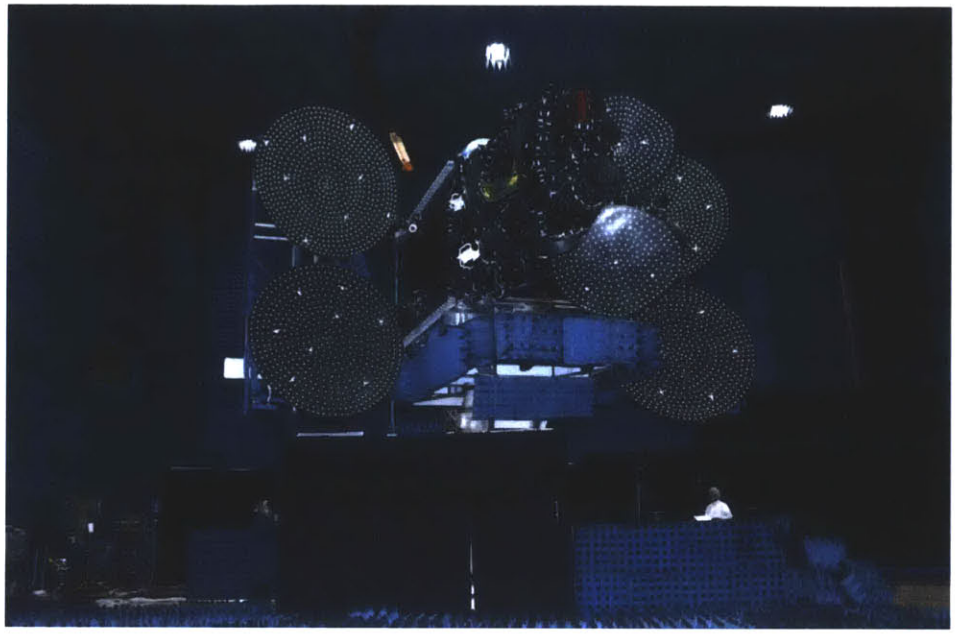

Figure 3-1: Intelsat 30 satellite during testing at Space Systems/Loral in Palo Alto, CA. Image Credit: Space Systems/Loral [121].

### Inmarsat

For this research, we also partnered in 2011 with Inmarsat, a UK-based telecommunications company, operating fleets of GEO ComSats since 1979 [57]. We have analyzed over 22 years of archived telemetry from 10 satellites from three fleets (different manufacturers). The data acquired includes SSPA current and temperature telemetry, solar array power and total bus loads, and anomaly and SEU lists.

W. Lohmeyer conducted a thorough analysis of 16 satellites from two Inmarsat fleets [75, 76]. Since 1996, the satellites have experienced twenty-six SSPA anomalies. SSPAs are key components in satellite communication systems, used to amplify the uplink signal received by the satellite from the ground (which is degraded due to path loss, etc.) before retransmitting the downlink signals for the ground users. A thorough analysis of the timing of SSPA anomalies with respect to the environment can be found in Lohmeyer et al. 2012 and 2015 [77, 78].

Figure 3-2: Artist's conception of Inmarsat's Global Xpress satellite. Image Credit: Inmarsat [57].

### 3.1.2 Space Weather Data

Space weather datasets are selected from multiple sources based on the relevant hazards in GEO discussed in Section 1.1.1. This analysis uses energetic particle data from GOES, geomagnetic storm indices from the WDC for Geomagnetism in Kyoto, sunspot daily averages from the World Data Center in Brussels, and solar wind data from ACE. For all datasets, we collect data over the entire span of the GEO ComSat telemetry (from 1991 to 2015), except the data from ACE, which became operational in 1998.

#### Energetic Particle Data

GOES is operated by the United States' National Environmental Satellite Data and Information Service (NESDIS), providing Earth severe storm tracking and meteorological data. In addition, GOES supports space weather forecasting (see NOAA Space Weather Prediction Center (SWPC), using the Solar X-ray Imager (SXI) and the Space Environment Monitor (SEM), which provides continuous[1] measurements

[1]Complete GOES outages are rare since there are typically three operational satellites making measurements on orbit at any time [92], though sensor saturation during large storms can affect

Table 3.1: Summary of telemetry acquired and analyzed from Intelsat and Inmarsat.

| | **Intelsat** | **Inmarsat** |
|---|---|---|
| Headquarters | Washington, D.C. | United Kingdom |
| Number of Satellites | 21 | 10 |
| Number of Bus Types | 4 | 3 |
| Time Range | 1996-2015 | 1991-2012 |
| Years of Data | 20 | 22 |
| Telemetry Obtained | TWTA and SSPA current and temperature telemetry; solar panel current, total bus power, shunt loads; magnetometer measurements | SSPA current and temperature telemetry; solar panel current, total bus power; anomaly and SEU list |
| Telemetry Resolution | Hourly, minutely, minor frame (<1 minute) | Hourly |
| Data Quantity | >0.5 TB | >500 MB |

of the energetic particle and magnetic environments in GEO. In operation since the mid-1970s, the GOES satellites have been a primary source for public, military, and commercial space weather warnings [19, 120].

The SEM consists of three magnetometers, an X-ray/extreme ultraviolet sensor (XRS/EUV), and an energetic particle sensor/high-energy proton and alpha detector (EPS/HEPAD). This analysis uses data from the EPS/HEPAD, which measures the energetic particle flux.[2] Specifically, the instrument consists of two energetic proton, electron and alpha detectors (EPEADs), a magnetospheric proton detector (MAGPD), a magnetospheric electron detector (MAGED), and a HEPAD [19]. We use the GOES EPS 2 MeV electron flux channel data (five-second resolution). Additionally, we use the GOES EPS P4 proton flux channel, which measures protons between 15-40 MeV [19, 120]. We have collected data that spans the entirety of the ComSat telemetry (from 1996 to 2015), which can be obtained from the NOAA National Geophysical Data Center [93].

availability.

[2]Flux is the number of particles through a unit area per unit time. Units: particles-cm$^{-2}$s$^{-1}$sr$^{-1}$.

### Geomagnetic Indices

The Geomagnetic Equatorial Dst Data Service is hosted by the WDC for Geomagnetism[3] in Kyoto, Japan [146]. Several types of geomagnetic indices (Dst, Kp, Ap) are calculated at the center that are then verified and archived for public access. This database was used for acquiring values of Level 2 Dst and Kp for the length of the ComSat telemetry for determining dates for severe geomagnetic space weather events between 1991 and 2015.

### Solar Environment

For the solar environment information, we use daily sunspot numbers from the World Data Center Royal Observatory of Belgium in Brussels [147] to compare events with the strength of the solar cycle (for which the sunspot number is a proxy, as described in Section 1.1.1 and Appendix A. The data is collected from a network of observing stations. Three terms, $g, s, K$, are used to calculate the relative International[4] sunspot number $R = K(10g + s)$ [31]. The observing stations record the number of sunspot groups $g$ and the number of distinct spots $s$. The scale factor $K$ allows for differences in the observing station's equipment and conditions.

The ACE satellite makes measurements of the solar wind, including the speed, density, temperature and composition. The ACE Real-Time Solar Wind System (RTSW) consists of four instruments: Energetic Ion and Electrons (EPAM), Magnetic Field Vectors (MAG), High Energy Particle Fluxes (SIS), and Solar Wind Ions. We predominately examine measurements of the solar wind speeds from the Solar Wind Electron, Proton, and Alpha Monitor (SWEPAM). The solar wind speeds also provide evidence for magnetopause compression. If the solar wind speeds, and therefore pressure, are high (600-800 km/s) then the magnetopause is likely to compress, placing GEO ComSats outside of the magnetosphere where they are unshielded from the harsh

[3]The Data Analysis Center for Geomagnetism and Space Magnetism is a part of the World Data Center for Geomagnetism and consists of the Data Center and the University of Kyoto's Graduate School of Science.

[4]The International Sunspot Number is similar to the Zurich relative sunspot number, originated by Rudolph Wolf in 1848 [144].

space weather environment [4].

The ACE satellite has provided operational data since January 1998 and is located at the first Lagrange point (L1), approximately 1.5 million km from the Earth, always observing local dayside. A benefit of the ACE satellite's stationary location is that in combination with the solar wind speeds, one can calculate the time at which the solar wind carrying energetic particles should impact Earth [92].

### 3.1.3 Satellite Anomaly Data

In addition to space environment measurements, we also examined dates and types of reported satellite anomalies in or near GEO at the same time as events detected in the spacecraft telemetry. Unfortunately, while there is much interest in the creation and maintenance of a robust, centralized repository of satellite anomalies, it does not yet exist [46, 95] due to sociopolitical and economic norms and motivations of the industry's constituents [26]. There exists a handful of anomaly lists maintained by individuals that were used in this analysis.

Starting in 1983, Dr. Joe Allen began collecting and maintaining the largest publicly available database of satellite anomalies at the Solar-Terrestrial Physics Division of the National Oceanic and Atmospheric Administration (NOAA) National Geophysical Data Center (NDGC). The database, which is no longer active – with contributions slowing down in 1990 and eventually ceasing (last updates posted in December 1993) following Allen's retirement – contains over 5,000 entries[5] [6, 7].

Satellite News Digest (SND), an industry website, collects information and analyses about satellites, cataloging information for a variety of purposes [68]. SND's assembled information is largely available to industry members through a subscription, which allows access to SND's anomaly records, which are maintained by Peter C. Klanowski, a Germany-based freelance writer. Since 1994 (with an English version starting in 1997), SND has maintained an archive of publically available satellite failure information.[6] Klanowski admits that the database is sparse and likely does

[5]Data can be found at the NOAA GDGC: http://www.ngdc.noaa.gov/stp/satellite/anomaly/doc/anomalies.txt
[6]SND satellite anomaly records can be found here: http://www.sat-nd.com/failures/

not contain many of the anomalies that are likely to have occurred.

## 3.2 Acquired GEO ComSat Telemetry: Examples and Challenges

The GEO ComSat data is a time-series of measurements from sensors and instrumentation on-board the spacecraft. Each measurement is time-tagged and transmitted to the ground for analysis. This section displays selected examples of the acquired GEO ComSat telemetry, which illustrates some of the challenges with this dataset, such as the choice and availability of telemetry resolution, missing data, and noise, are considered in Section 3.2.2.

### 3.2.1 Examples

A plot of a nominally performing SSPA from Inmarsat can be found in Figure 3-3. A plot of thermistor telemetry from the same amplifier can be found in Figure 3-4. The time resolution for both Figures is hourly and had no reported anomalies (SEUs, etc.). In Figures 3-5 and 3-6, current telemetry from an Intelsat SSPA is plotted with two different resolutions, hourly and minutely, to demonstrate the noise difference with sampling choice.

In general, telemetry resolution (or the time between samples) depends strongly on the phase of the mission and what is being measured. For example, propulsion tank pressures may need to be sampled at a higher frequency during maneuvers, while the payload On/Off status transmitted less frequently during a maneuver may be satisfactory. The frequency of telemetry sampling and the number of parameters telemetered impacts the required bandwidth (driven primarily by data rate and choice of modulation scheme), compression, formatting, storage, etc. [141]. Therefore, slower sampling (more time between measurements) is chosen when possible over faster sampling rates. For housekeeping data (the focus of this thesis), infrequent intervals of typically 30s to 2 minutes, up to 1 hour, are usually sufficient [42]. The

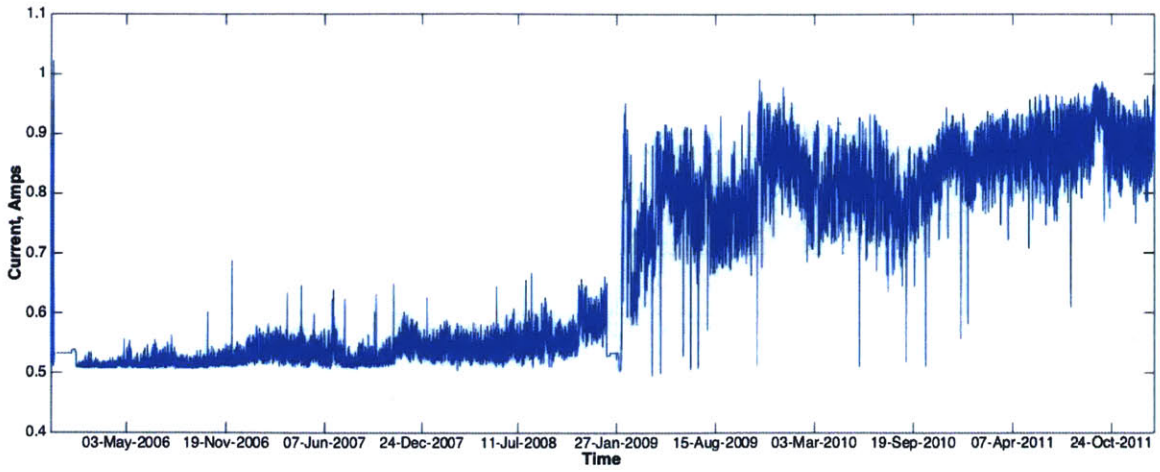


Figure 3-3: Nominally performing solid-state power amplifier from an Inmarsat satellite.

GEO ComSat telemetry acquired has hourly, minutely, and minor frame (sub-minute) sampling.

### 3.2.2 Challenges

The key challenges associated with the GEO ComSat telemetry are the acquisition and management of the telemetry, and the noise in and resolution of the telemetry.

#### Data Acquisition and Management

Access to space weather data as well as satellite telemetry has been identified as the first step to understanding to what extent space weather is related to the root cause of anomalies [94]. However, access to space weather and satellite telemetry is often challenging, especially in the case of satellite telemetry, and often impossible to get both sets of data for the same time period. Both datasets are necessary to quantify space weather effects [10, 131].

Space weather products of interest, as described in Section 3.1, are publicly available for the most part. However, they are generally limited in their utility due to sometimes large spatial separations from the satellite of interest [96]. In the case of GEO ComSats, GOES satellites are also in GEO, but can be located more than 100

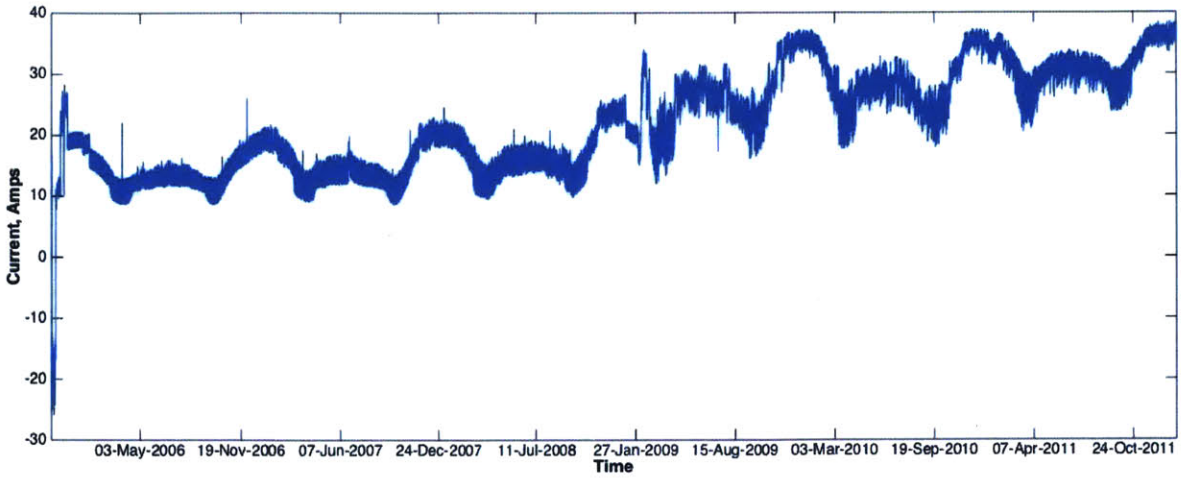


Figure 3-4: Nominally performing thermistor in the amplifier payload from an Inmarsat satellite.

degrees in longitude from the GEO ComSat.

The challenges with satellite telemetry can be summarized in three main areas: access, management, and interpretation of data. Satellite telemetry is rarely made public. The data is proprietary, and access is limited due to satellite operators' concerns about competitive advantage [26, 95]. To gain access to telemetry from Inmarsat and Intelsat, we have established partnerships to assist with anomaly root cause analysis and fault investigations. This has required spending weeks at both Intelsat and Inmarsat to learn about specific company operations and about how telemetry is managed (cataloged, designated, etc.).[7]

Once selected, the quantity of data poses a logistical challenge. The GEO ComSat telemetry from Intelsat alone, from only a select number of components and satellites, totals over 0.5 TB. This quantity of data cannot be stored on a typical computer. In addition, it must all be encrypted (at the request of the operating company). We have chosen to store data on encrypted hard drives, and have to switch in and out hard drives depending on which dataset we need access to (due to limits on hard drive capacity). We have developed scripts to interact with the databases. Clever organization of data, database management and tools to interface with the data are

[7]The telemetry streams have designations that are not often clear what the sensor is measuring, for example. This has required extensive iteration with the companies to determine which telemetry streams are of interest to us.

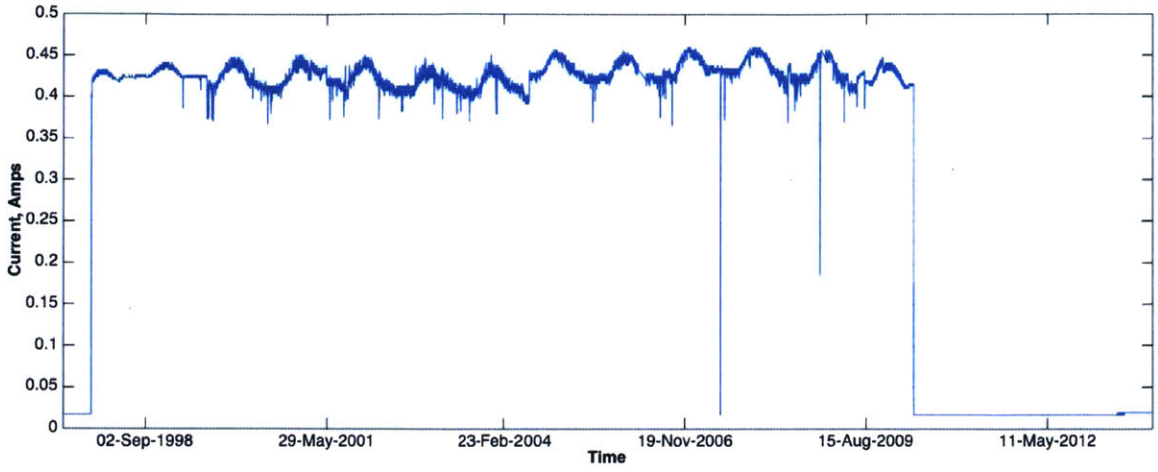


Figure 3-5: Solid-state power amplifier from an Intelsat satellite, hourly resolution (same amplifier as Figure 3-6).

non-trivial, time-wise.

Lastly, interpreting the telemetry presents a key challenge. Without knowledge of where the telemetry specifically comes from (*i.e.,* physically on the spacecraft or in the component) or of how the data is collected and recorded, telemetry interpretation is problematic. We rely on the operators and manufacturers to provide this information, though it is often difficult to acquire. Operators are typically not affiliated or collocated with the manufacturers of the satellites, and specifications, such as technical drawings, may not be in the operators' possession or at their discretion to share or distribute.

### Noise and Resolution Challenges

As seen in Section 3.2.1, the telemetry is noisy. Events detected by the algorithms could be anomalous events or sensor noise. Disentangling the two is challenging, and both types are detected with the current event detection scheme presented in this thesis. Missing data could be due to data dropouts (transmission or recording errors, etc.).

Sometimes it is unclear which specific component on-board has had an issue because not every component may have a telemetry feed. As mentioned in Section 3.2.1,

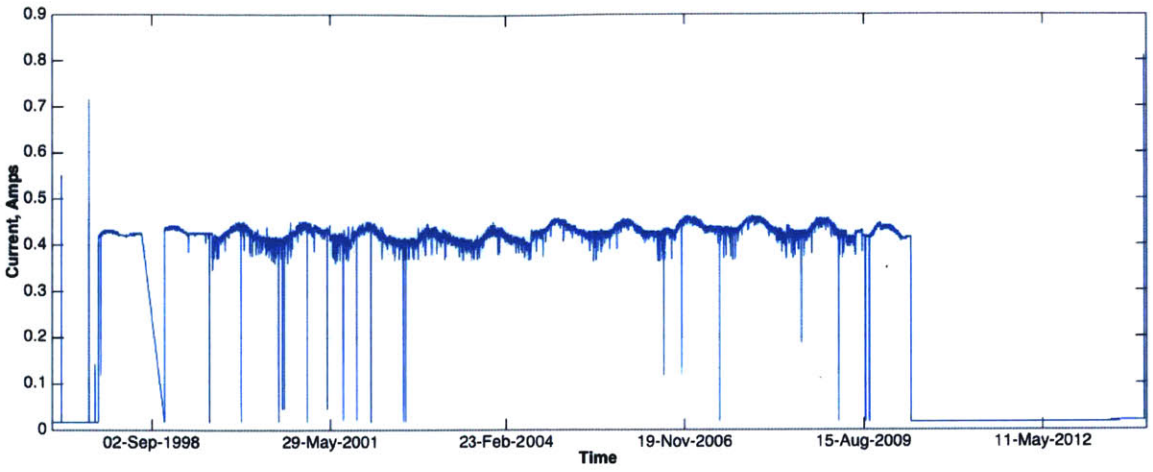


Figure 3-6: Solid-state power amplifier from an Intelsat satellite, minutely resolution (same amplifier as Figure 3-5).

satellites have finite resources for data-handling. As a result, telemetry is collected from critical components and, thus, cannot convey the entire picture of the satellite system [141].

Telemetry resolution limits the types of anomalous issues one could detect (see Nyquist Sampling [118]). For example, maneuvers for GEO ComSats can last several hours and up to a couple of days depending on the maneuver, so minutely and hourly resolution is likely sufficient for detecting these events. However, electrostatic discharge events happen in fractions of a second, so minutely sampling will not be able to detect the event in progress. The resulting degradation may be able to be detected, but not the event itself.

# Chapter 4

# Algorithm Analysis and Results

## 4.1 Algorithm Descriptions

The algorithms developed to date aim at detecting atypical features, called "events" in this thesis, in the GEO ComSat telemetry. The algorithms include a method for detecting transient events (or "spikes", jumps, drops) and for detecting change points in the GEO ComSat telemetry. Figure 4-1 shows an example of both types of events. Each event detected has an event date and an event score, which is a metric for the magnitude of the event relative to what is "normal" in the telemetry. The scoring metrics are discussed in more detail in the sections that follow.

We use statistical techniques to find transients and change points. There is no imposed domain knowledge: the algorithms do not contain or impose any component- or satellite-specific parameters or thresholds. There is no assumption about the underlying distribution of the telemetry, and no training data required. More details and rationale behind these choices are provided in Chapter 2. In Sections 4.1.1 and 4.1.2, a description of the algorithm, parameters, and applied telemetry examples are provided for both transient and change point detection algorithms, respectively. A summary description of both algorithms is given in Table 4.1.

For both algorithms, non-parametric statistical parameters are used (median, quartiles, etc.). The median is chosen as the statistical metric over mean. Mean assumes a normal distribution of the data, which is rarely ever the case, and has been

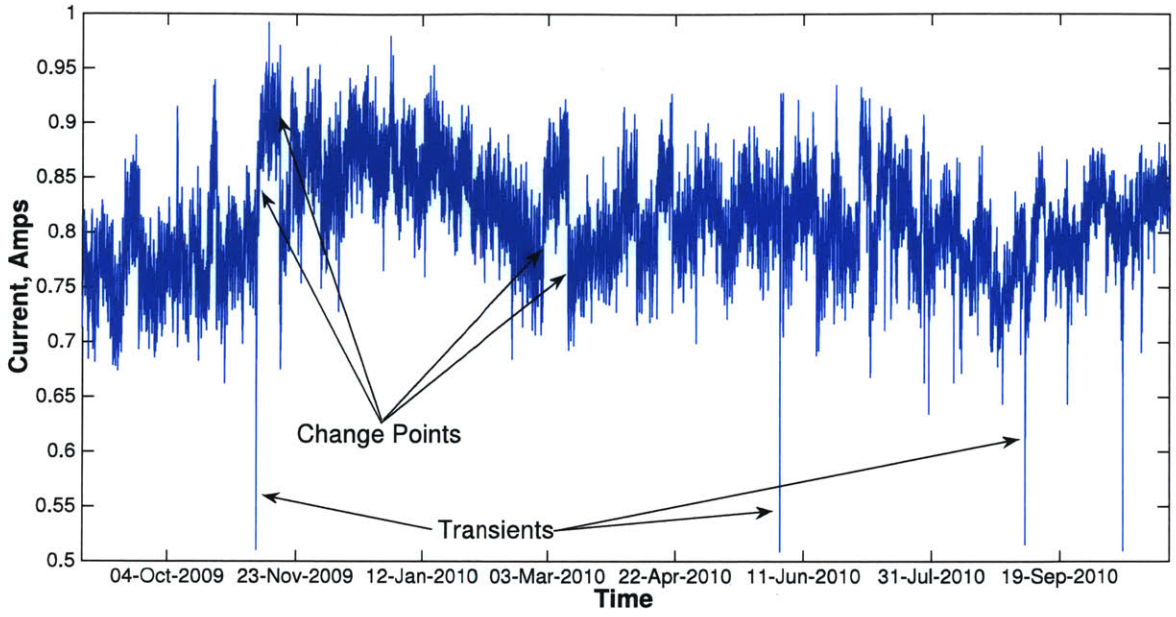


Figure 4-1: Plot of SSPA telemetry. The large transient events and change points are marked as examples of events detected by the two algorithms.

shown to be true for this dataset using a KS-test. Median is more robust to outliers, which is advantageous if the outliers are what we are interested in detecting.

### 4.1.1 Transient Event Detection

#### Description

Transient event detection is based on the Tukey Method, relying on statistics of the dataset to identify deviants [133, 137]. However, the data is segmented into bins (or windows) that allow for the definition of "normal" to change over the dataset. In the case of this work, the window is shifted along the dataset, comparing each telemetry data point to the rest of the data points in the window. This is very similar to the lightweight methods used by Hewlett-Packard in their online anomaly detection in data center management, who also use a variant of the Tukey method [137].

The transient event detection method uses a constant segmentation scheme (same duration window sizes), with a choice of 7-day windows. One orbit of a GEO satellite is 1 day, so 7 days allows for any possible orbital periodicity to be (somewhat) mit-

Table 4.1: High-level description of transient and change point event detection algorithms.

| | **Transient Event Detection** | **Change Point Event Detection** |
|---|---|---|
| *Approach* | Use single sliding window | Use two adjacent windows, slide windows one data point at a time |
| *Detection* | Each telemetry data point is compared to the local median | Compare median between two adjacent bins |
| *Event Scoring* | Number of standard deviations the telemetry data point is from the local window median | Percent change in median between two adjacent bins |

igated. The telemetry resolution considered in this study is hourly, so this equates to 164 data points per window. A discussion of the event detection sensitivity to window duration/size is provided in Section 4.4

Each telemetry data point is compared to the local median. For each data point, the date and number of standard deviations from the local median is recorded. The number of standard deviations is the event score. Selecting the events that have the highest event scores (those that "deviate the most") or selecting the events with scores higher than some threshold, allows for the user to input their domain-specific knowledge, if they so desire. But, this is not necessary for the detection of events.

### Examples

In Figure 4-2, the transient events detected by the algorithm are marked on an example of SSPA telemetry. The event dates are plotted with standard deviation (in purple, right y-axis) and overlaid with the raw telemetry (in blue, left y-axis) for greater than 3 standard deviations from the "local median" (*i.e.*, 99.73% of the values lie within 3 standard deviations of the bin median). The transient event identification method detects all noticeable spikes, performing as intended.

Figure 4-3 shows another example of amplifier telemetry with transient events detected. This figure shows the entire dataset in the top panel (2006 to 2011) and

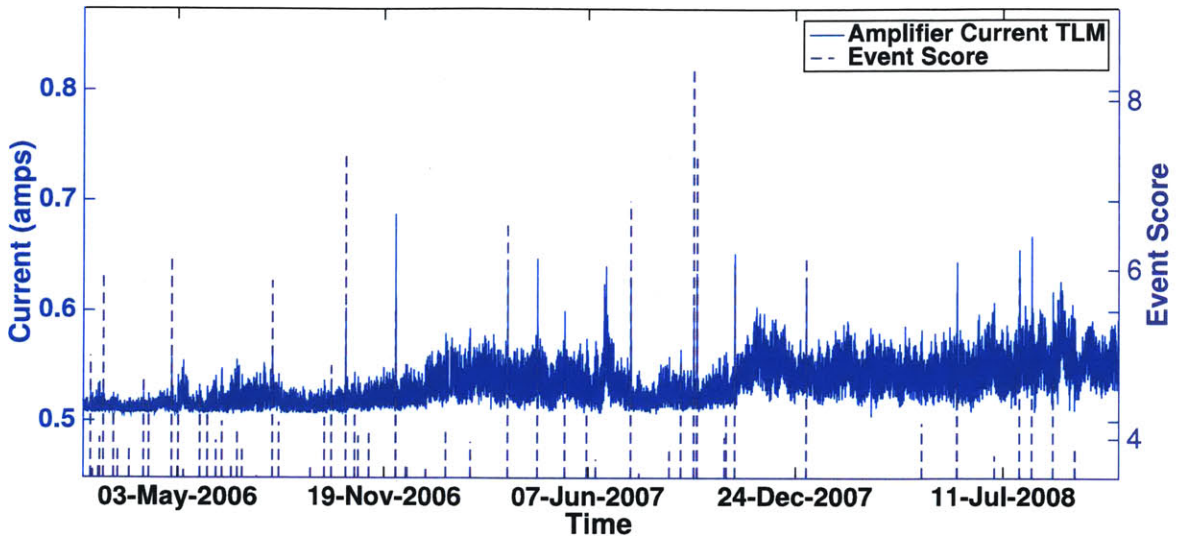


Figure 4-2: Transient events detected by algorithm on a SSPA telemetry stream.

a zoomed in region from December 2007 to October 2008. There are more events detected in the first half of the data (210 spikes detected before January 2009) than in the second half of the data (115 spikes detected after January 2009). This is because the standard deviation in the data is small (0.02276) prior to a change between December 2008 and February 2009. The data become noisier after 2009 and also contain larger changes in median. This change is seen across all Inmarsat datasets examined and may be indicative of a system-wide internal and/or external effect for those satellites. Given this scenario, a data point need not deviate from the local median by as much in the earlier half (pre January 2009) as it must in the latter half of the data (where the standard deviation is 0.08156) to be considered a transient event.

### 4.1.2 Change Point Event Detection

#### Description

Change point detection is prevalent in industries including finance, medicine, and sociology (see Section 2.3.3). As a result, there have been many papers on change point detection, such as those on climate change detection, genetic time series analysis, and

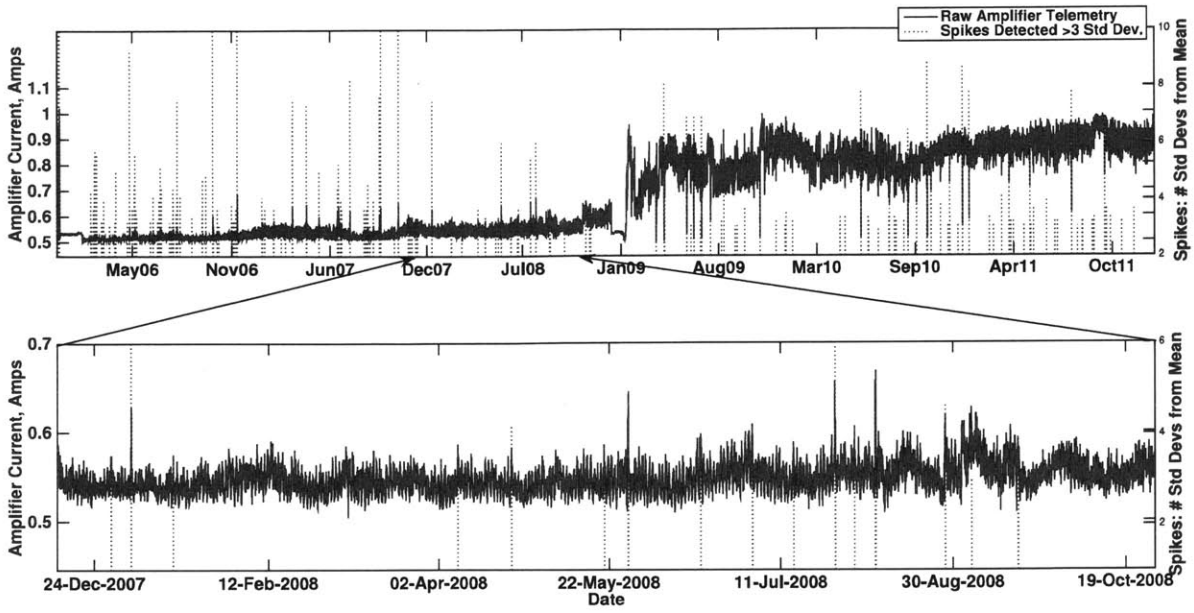


Figure 4-3: Transient event detection in amplifier telemetry. Spikes detected (in purple) for lifetime amplifier current telemetry from an SSPA for greater than 3 standard deviations from the local median. The left y-axis notes the amplifier current in Amps, and the right y-axis notes how many standard deviations the detected spike is from the local (7-day) median. Bottom: Zoomed in section from December 2007 to October 2008, demonstrating the algorithm's ability to identify spikes from the local median.

intrusion detection in computer networks [106, 137, 138, 149]. A common way to detect the change points and determine trends in time series data is by representing the data using Piecewise Linear Approximations (PLAs) (or, Piecewise Linear Representations (PLRs)) [115]. We use PLAs and approximate the data in bins (or windows). The statistics, such as the median, of each bin are compared. Bin size selection, or segmentation, is an active area of research [65, 66], and will be explored in future development of the telemetry event identification algorithms. The current method does not require "smart" binning techniques due to an optimization of the change point method (using a moving window technique) [67], as described below.

The change point detection algorithm employs an optimization scheme for finding the events, or "change dates." The data is initially segmented into 7-day windows (or "bins") and the weekly bin statistics (median, standard deviation, etc.) are computed.

For bins that show large changes in median between adjacent bins, an optimization routine is employed using a combination of two moving windows, one data point at a time (telemetry is in hourly resolution) to maximize the difference in the median between two adjacent windows in the local time frame of the originally large change in median. When the change in median is maximized locally, the date of the "event" is recorded as the boundary between the two moving windows.

The algorithm reports the largest changes in median, numbered with their change value in descending order. An example of a section of the amplifier telemetry after median change detection and optimization can be found in Figure 4-4. In general, we allow the algorithm to report more changes in median (*e.g.,* 30 changes detected) than we expect to be significant for the dataset. The significance ranking is determined by the magnitude of the change in median at the event date. The event date with the largest change in median is "#1"; the second largest is "#2", etc. As a result, if the user wants, when compiling all events together, there is a range of median change event dates ordered by significance, from which one can then select a minimum threshold after evaluating the entire dataset, *i.e.,* we do not want to restrict an amplifier, for example, to only detecting 15 events if many other amplifiers or components have 20 or more events detected, and we do not want to have the algorithm identify 15 event dates from a second amplifier if it only 10 have notable changes in median.

### Examples

The median change detection method successfully detects median changes identified by visual inspection, as seen in Figure 4-4. The large change identified in Section 4.1.1 as occurring in January 2009 is, indeed, detected and identified and is ranked #2 for the amplifier. The sharp drop in current at the very beginning of the telemetry is ranked #1. In Figure 4-4, the slight change seen by eye between the #9 ranked event and the #12 ranked event does not have a large enough change in median to be ranked in the top 30 events selected. For example, if the number of events to detect is increased to 40, the change between the #9 ranked event and the #12 ranked event is detected and ranked #39. The transient detection method did identify the spike

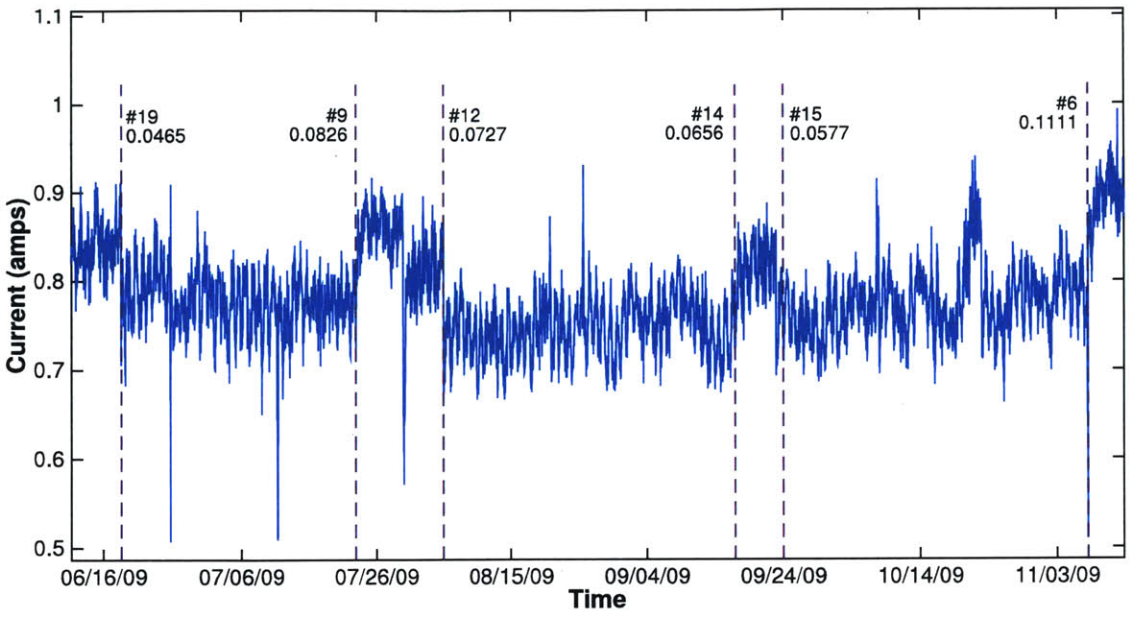


Figure 4-4: Median change detection method. Amplifier telemetry (blue) zoomed into a region (June 2009 - December 2009) with the detected median changes (dashed purple) using weekly bins. The method ranks the events (numbered) by the magnitude of the difference in the median, the value of which is provided below the numbered rank in this plot.

between the #9 ranked event and the #12 ranked event.

While we anticipate that users may want to incorporate weighting factors on the ranking system based on system knowledge or based on multi-component assessments, we have not yet included component- or spacecraft-specific factors into the event ranking process. In addition to the raw change in median, the method also reports the percent change in the median. This is useful when combining results from components that have different ranges of operational values. For example, current telemetry may exhibit changes in median on the order of tenths of an Ampere. Temperature data may exhibit changes on the order of many degrees Celsius.

## 4.2 Findings

The approach to fault detection and environmental sensing for the satellites is to use the algorithms to find atypical events in satellite telemetry. As discussed in

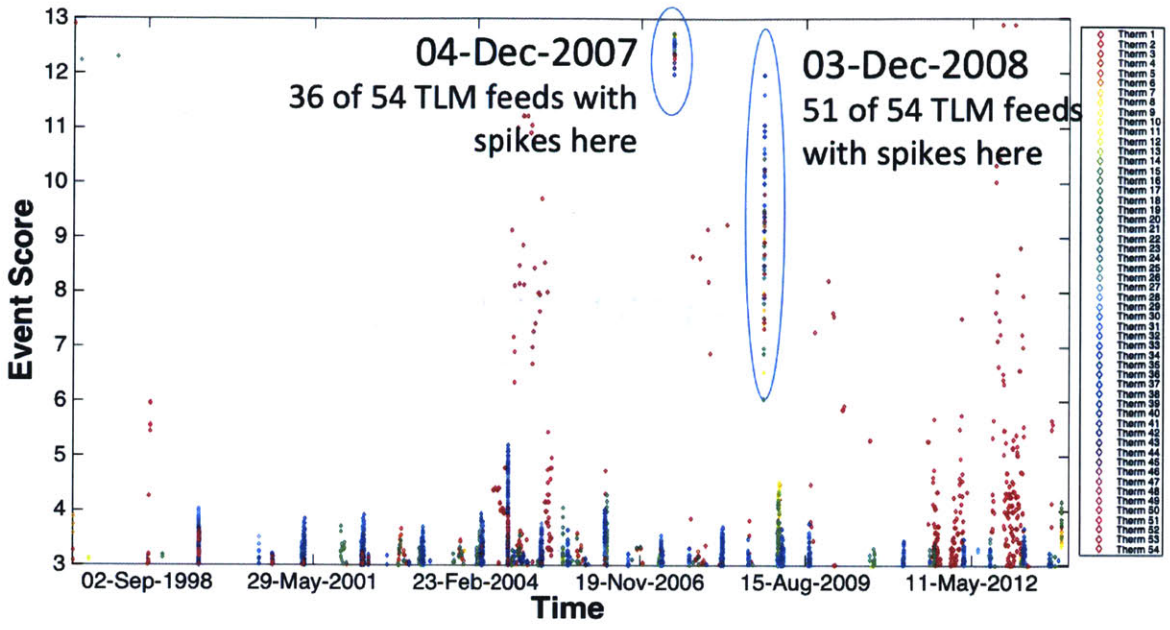


Figure 4-5: Events detected in 54 thermistor telemetry streams in one satellite. Each thermistor is a unique color.

Section 2.4, the algorithms are applied to individual telemetry streams. The events are compiled for a particular satellite component, for one satellite, and for multiple satellites (*e.g.*, for a fleet). The application of the algorithms to individual telemetry streams is shown in the examples in Section 4.1. The following section compiles the events at the different layers of abstraction.

We find certain event dates when many if not all the components of a particular subsystem or satellite have an event detected. These event dates may be indicative of system-level or environmental-level events. We compare the events to known spacecraft activity and to known space weather events and indices.

### 4.2.1 Results for Individual Types of Components

When comparing the events detected for a type of component on a satellite, we find clusters events at dates that are clearly not random. For example, for a set of thermistors on one satellite (54 telemetry feeds), we have plotted the date and event score for each telemetry stream, each thermistor with a different color. Figure 4-5 shows that the transient events are not random: there are dates where there are large

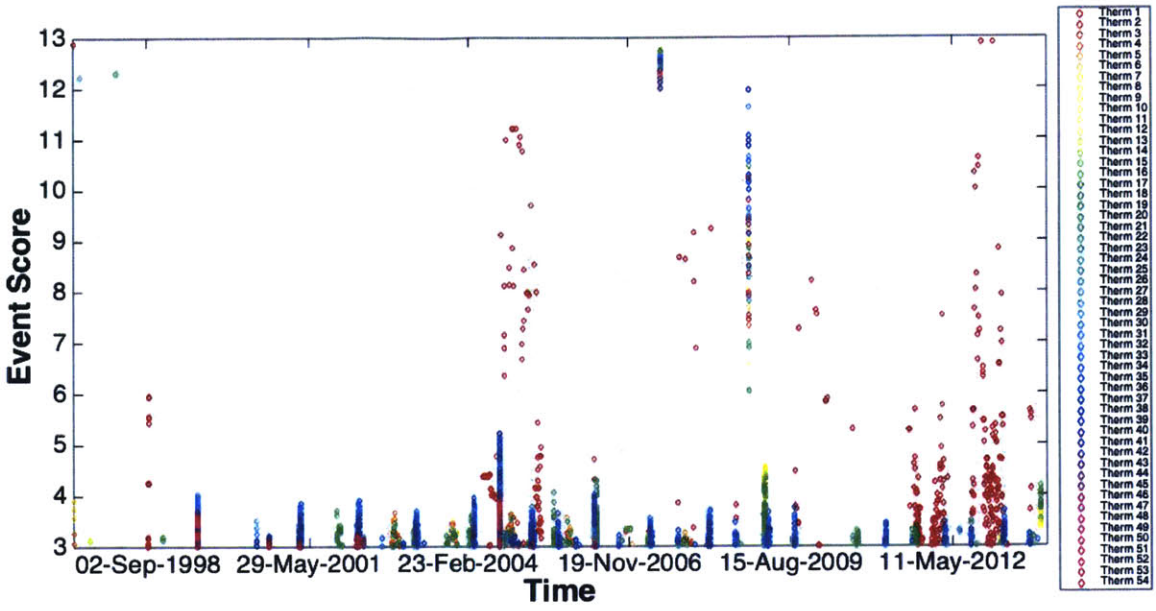


Figure 4-6: Events in thermistor telemetry annotated with eclipse seasons. The light green shaded regions are spring eclipses and the light red regions are fall eclipses.

events across many, if not all, of the telemetry files. Large events (dates when many telemetry streams have high event scores) in December 2007 and December 2008 are annotated in Figure 4-5. This suggests there is some relationship between the transients in the telemetry and system-level events, whether internal to the spacecraft or due to external environmental influences. There are some thermistors that do not show clustering of the other thermistor events, such as thermistors 1 and 2 (in red and red-orange).

The clustering of event dates with event scores between 3 and 4 appears to have a rough periodicity. This periodicity is likely explained by the eclipse seasons of the satellite, which are marked on the plot in Figure 4-6. The events appear to be related to moving in and out of eclipse. It should be noted that the largest events (highest event scores) and thermistors exhibiting dispersion do not appear to be associated with the eclipse seasons.

The dispersion exhibited by the first two thermistors in Figure 4-5 (shown in red and red-orange) could be due to the physical locations of the thermistors with respect to the others. The majority of the thermistors used in this study are from

the high-powered amplifier payload. Thermistors 1 and 2 are from the propulsion system, and are located near the thrusters. The wide spread in 2004 shows up in other components' event analyses as well.

### 4.2.2 Results for One Satellite

Compiling the events from all telemetry streams in the dataset for one satellite, we also find that some of the top events for different components occur on the same (or similar) dates. The compiled events from all amplifier and thermistor telemetry we have obtained from one satellite, totaling 185 telemetry streams, is show in Figure 4-7. The event scores are summed on each day for both types of components. There are event dates that clearly stand out. The top events (dates with the highest summed event scores on that day) are marked with purple triangles.

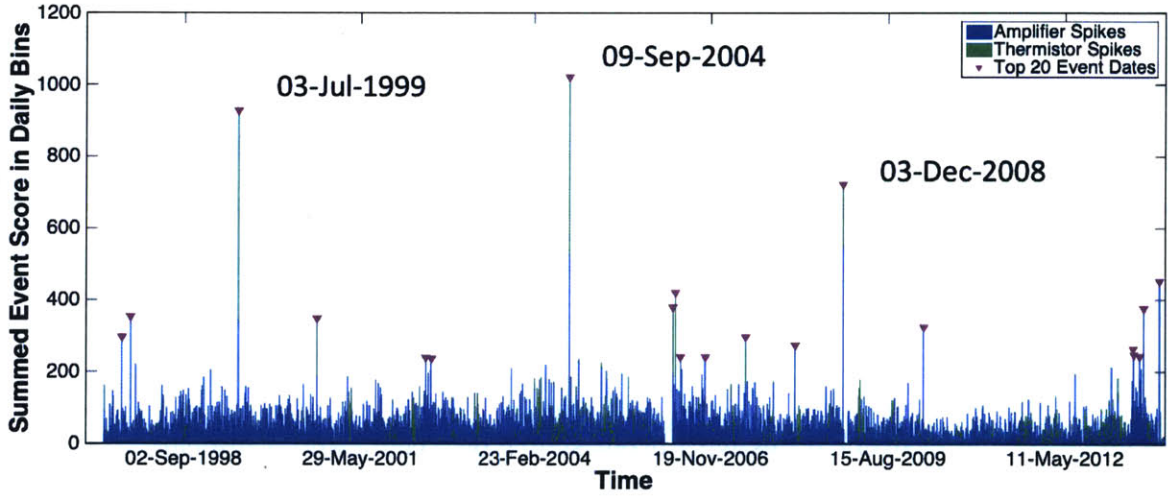


Figure 4-7: Summed event scores for each day for 185 telemetry streams from one satellite. The blue bars are the summed event scores for the amplifier telemetry events and the green bars are for the thermistor telemetry events. The two types are stacked so that the top events between the two component types are shown. The top twenty events (dates with the largest summed event scores) are marked with purple triangles.

Examining the top ten events from each of the two component types, we find that three of the ten top events are on the same date: 03-July-1999, 09-September-2004, and 03-December-2007. These events are noted on Figure 4-7. The occurrence of

these events indicate possible system-level events. These event dates are compared to known space weather and spacecraft activity in Section 4.3.

The same event detection algorithms were deployed on the other satellites in the dataset. We find that there are dates where the top events from one satellite coincide with a top event from another satellite. From one satellite, we see a top event date of 03-December-2008 (as shown in Figure 4-5). In another satellite, we see a top event data of 04-December-2008. When examining the events, a daily binning scheme was selected, so these top events only separated by a day could be related. We investigate this further in Section 4.3.

## 4.3 Event Analysis

### 4.3.1 System-Level Event Investigation

For each satellite in the analysis, we have investigated the top reported events. We have compared the dates to known space weather activity: GOES >2 MeV electron flux (daily fluence), GOES >10 MeV proton flux (daily fluence), the Kp index (measure of the geomagnetic activity), and to other notable events, such as Coronal Mass Ejections (CMEs), interplanetary CMEs, and meteor showers. Figure 4-8 shows the events and event scores plotted with space weather metrics. We have also compared the event dates to known spacecraft operations and to other reported satellite anomalies. We have summarized the findings from one satellite in Table 4.2. A more detailed table of the event analysis can be found in Appendix B.

For each satellite that had a maneuver during its lifetime, the maneuver is detected as one of the top 5 events for each of the satellites. This is a significant finding because this information could be useful for a group who is interested in a satellite's activity and listening in on a satellite's telemetry, such as for a SSA application.

For five of the satellites, we have Single Event Upset (SEU) dates and times. We find no statistically significant relationship between the SEUs and the events detected by the algorithms. There are a few instances where the event detected in the telemetry

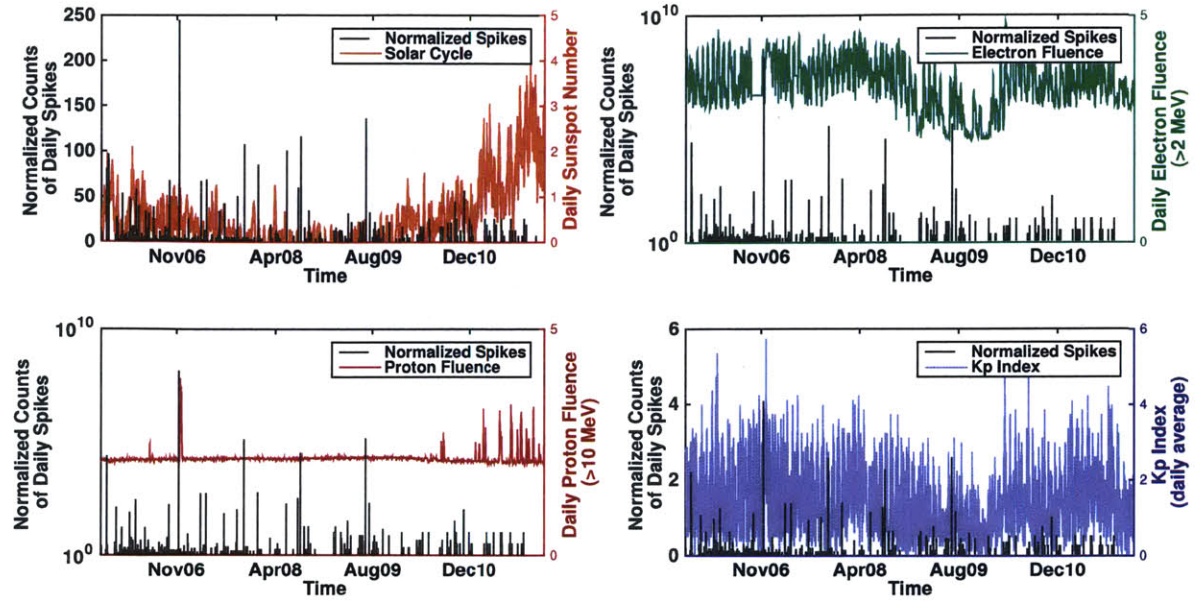


Figure 4-8: Plots of the daily summed event scores for all telemetry streams from one satellite (199 telemetry streams) compared to space weather metrics: sunspot number (top left), daily electron fluence in GEO from GOES (top right), daily proton fluence in GEO from GOES (bottom left), and Kp index (bottom right).

occurs within a couple of days of an SEU (see Table 4.2).

### 4.3.2 Environment-Level Event Investigation

#### December 2008 Events

As mentioned in Section 4.2, there are two satellites that have their largest events at the system-level only separated by one day, referred to as Satellite A and B for simplicity. Upon closer investigation, the events from Satellite A and B occur at 03-Dec-2008 23:25:59 and 04-Dec-2008 04:59:59, respectively[1]. Telemetry from each satellite spans over a decade, so it is unlikely that it is a coincidence that these events are unrelated. It could be indicative of an environment-level event that has been detected.

We examined the locations and separation of these two satellites on orbit (infor-

[1]Recall, this analysis is using hourly telemetry, so the times listed here is not exact to the digits reported. The time reported in this analysis is the time the telemetry was sampled that hour.

Table 4.2: Top event date analysis for one satellite. The event dates are compared to the space weather environment, spacecraft operations, and reported spacecraft anomalies. More information can be found in Appendix B.

| **Top Event Dates** | **Space Environment** | **Spacecraft Operations** | **Other Reported Anomalies** |
|---|---|---|---|
| 03-Dec-2008 | None, quiet | Transponder SEU on Dec. 7 | Thruster anomaly with GOES-12 |
| 09-Sep-2004 | Fast solar wind from coronal hole arrived at Earth 6-7 Sep 2004 | None | Thaicom outages 12-Sep-2004 |
| 02-Jul-1999 | None, quiet | None | Echostar IV fuel system anomalies in July 1999 |
| 28-Oct-2013 | Handful of powerful CMEs starting Oct. 25, several associated X-class flares | None | Unknown |
| 04-Nov-1997 | None, quiet | Maneuver in progress | Unknown |
| 02-Jul-1999 | Moderate Kp=4 | None | Echostar IV fuel system anomalies July 1999, ABRIXAS failure of onboard batteries |
| 28-Feb-2010 | 28-Feb-2010 large CME, not Earth-directed | Maneuver in progress, Transponder SEU Feb. 27 | AMC-16 further degradation of solar arrays early March 2010, GEO |

mation not revealed for proprietary reasons). Satellite A is located to the east of Satellite B. Satellite A is the first to experience the event, and then about five hours later, Satellite B experiences the major event (having moved eastward towards Satellite A's initial position). The time spacing between the locations is roughly two hours. The top events are recorded within 5 hours of each other. It seems very unlikely that these events are unrelated, and there is likely an environmental reason for the largest events for both satellites to occur within a few hours of one another. Further analysis is required to determine the cause of this potential environmental event.

### Events Compared to the Space Environment

We compare the high-energy electron fluence accumulated before the largest events. Build up of high-energy electrons can lead to charging of dielectric materials, potentially causing catastrophic discharges [18, 78]. Comparing the fluence accumulated 1, 7, 10, 14, and 21 days prior to the large event dates to a random Monte Carlo sampling of days, we find no statistically significant relationship between accumulated fluence and the events detected by the algorithms.

Roughly half of the events detected occur when there is a sharp increase in solar wind speed. This could be due to such events as the passing of a fast CME, from a coronal hole, or a slower CME being overtaken by a faster CME. Future work includes a more detailed investigation of the timing of the solar wind changes compared the event times though this is limited due to the lack of solar wind detection in GEO at the time of the event. To supplement, we will look into using solar wind propagation models, such as those in the Space Weather Modeling Framework (developed by the University of Michigan and supported by the Community Coordinated Modeling Center (CCMC)) [130].

## 4.4 Algorithm Performance and Sensitivity

### 4.4.1 Computational Resources

Since the transient detection method involves comparing each individual data point to local median, the execution time is expected to be linearly dependent on the size of the telemetry file. Running the method on our dataset confirms this expectation of a linear relationship between computational time and the number of data points. For example, for an Inmarsat telemetry file with hourly resolution (6.14 years, 1,284,144 data points), the method takes 0.0721 s. For reference, the total time to run the transient detection method is 0.572 s on 18 telemetry files[2].

Running the change point detection method on our dataset shows a linear, nearly constant, relationship between execution time and number of telemetry data points. For example, for an Inmarsat telemetry file with hourly resolution (6.14 years, 1,284,144 data points), the method takes 0.576 s and the average time is 0.553 s for all telemetry files[2]. For reference, the total time to run the change point detection method on 18 telemetry files is 9.950 s.

### 4.4.2 Tunable Parameters

The algorithms currently sum event scores by day, summing the event scores for the 12:00 AM to 11:59 PM time period. This choice allows for a quick examination of data when over a decade of telemetry is analyzed. However, this choice leads to some discrepancies, like those discussed for the December 03-04, 2008 events. Therefore, this binning start time is a parameter, which is prompted for at the start of the routine. We have moved the summation start/end times by fractions of a day and found that the top event dates are still the largest in each run.

In addition, the duration of the summation window (1 day in this analysis) can be eliminated, and the resolution of the telemetry (hourly, for example) can be used for event score summing. This leads to binning of event scores by telemetry resolution,

[2]The transient and change point detection methods were run on a MacBook Pro version 10.9.5, 2.5 GHz processor, 16GB memory, MatLab version 8.4.0.150421 (R2014b).

but can be challenging when trying to detect environmental effects in satellites that are not spatially collocated.

For transient event detection, the bin size for comparing a data instance is the median over one week. For change point detection, the median is compared between one-week sets of data instances. This one-week duration is also considered a tunable parameter: the routine prompts the used for an integer number of data points as the window size (making it dependent on the data resolution). Similar to the choice of the start of a bin, we find no change in the results reported for the top events.

# Chapter 5

# Concluding Remarks

Knowledge of the space environment is key for the design, performance, and long-term operation and reliability of GEO ComSats, which are critical assets to communications, navigation, science, and defense industries worldwide. The algorithms presented in this thesis aim to identify events and trends in GEO ComSat telemetry, applying ranking metrics to single component telemetry streams, and compiling the events across multiple components, and across multiple spacecraft or fleets. Using space weather data for validation, the algorithms enable the telemetry to be used a "sensor" for the space environment.

We conclude with a summary of the algorithm work to date. We highlight key assumptions and weaknesses in the current algorithms and approach. We conclude with the near-term path forward for this project[1] and the future applications, impacts, and long-term benefits of the work started in this thesis.

## 5.1 Summary of Work

We have developed algorithms that identify deviations from normal, avoiding component- or satellite-specific conditioning. The current algorithms are capable of detecting transient events and change point events. We have presented preliminary results

[1]Future work is to be completed in A. Carlton's doctoral studies, funded by the NASA Space Technology Research Fellowship.

demonstrating detection of transient and change point events, finding the events noted by visual inspection along with subtle jumps and changes, and the reporting of events detected by their relative deviation from nominal.

We have built relationships with two GEO ComSat operators, Inmarsat and Intelsat, allowing us to consider a GEO ComSat dataset of 22 satellites, spanning almost two decades (1996 to 2015) in this analysis. We find both transient and change point events that occur in many or all of the telemetry files considered (GEO ComSat dataset), indicating potential system-level effects on certain dates. In addition, we find an event date that occurs in two satellites: 04-December-2007, which may be indicative of an environment-level event. We have considered the space environment, available operational information, and anomaly reports from other spacecraft in GEO. Futher analysis with the events detected is required to determine if a relationship exists.

## 5.2 Algorithm Assumptions and Vulnerabilities

### Non-Parametric Statistics

Non-parametric statistics are used in this analysis, which simply means that the statistics are not based on parameterized families of probability distributions (such as the commonly used normal distribution). We make no assumptions about the probability distributions of the variables being assessed. To verify that the data are not normally distributed, we tested the data with a one-sample Komolgorov-Smirnov test ("ks-test") [82]. The test rejects the null hypothesis at the 5% significance level that the data is normally distributed. Figure 5-1 shows the empirical cumulative distribution function (CDF) compared to the standard normal CDF.

The wider applicability and increased robustness of non-parametric tests comes at a cost: in cases where parametric would be appropriate, non-parametric tests have less power (*i.e.,* a larger sample size can be required to draw conclusions with the same degree of confidence). However, we do use standard deviations. This is because it is difficult to characterize the spread non-parametrically. Future work will examine

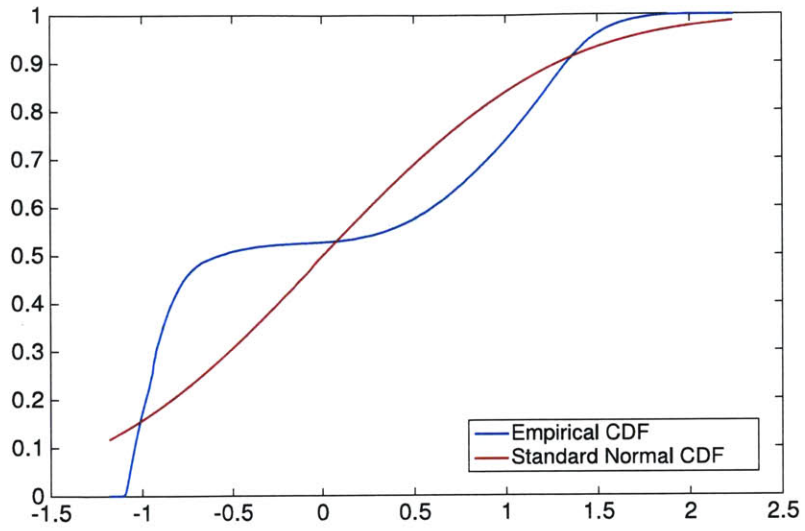


Figure 5-1: Empirical cumulative distribution function (CDF) compared to the standard normal CDF for a one-sample Kolmogorov-Smirnov test on an example telemetry stream. Telemetry streams from other components were also tested and yielded the same result: reject the null hypothesis that the data is normally distributed.

the use of quartiles, which is the basis of the Tukey method [133].

### Lack of Spacecraft Operational Data

A key weakness in this study is the lack of availability of spacecraft operational data. There many variables affecting telemetry, including the operational procedures and commanding of the components and spacecraft as a whole. Commanding may cause the telemetry to change, and we want to be able to identify these affects (to make sure we do not confuse them with other sources, such as the environment). We have acquired maneuver logs, which are used in the analysis in Section 4.3, but have been unable to acquire other operational information for proprietary reasons. For example, for the Inmarsat data, the changes in median may occur due to routine ground system reconfiguration.[2] Future work includes a continued effort to obtain the operational data.

[2]Personal communications with Inmarsat operators (July 2015).

#### Window Sizes and Binning

As discussed in Section 4.4, the choice of window size for change point comparison and transient event data instance comparison occurs for a window of 7 days. This is a tunable parameter, but it is an assumption for the analysis. This assumption was made based on the current data set: GEO ComSats orbit in a synchronous rotation with Earth, returning roughly every day. The window choice of 7 days allows for daily periodicity to be smoothed out over the median. Greater than 7 days may not allow for smaller events to be detected. This is a parameter we will explore as we expand our datasets.

#### Data Resolution

Currently, the majority of the data in our datasets have hourly telemetry resolution. This is a challenge and may prevent detection of events that occur on shorter time scales, such as electrostatic discharges. Future work includes acquired data sets with finer resolution.

## 5.3 Future Work

### 5.3.1 Path Forward

The path forward for this work is in the areas of increasing data for testing and validation, algorithm development, and considerations for integration into current operations.

#### Increasing the Telemetry Database

We are actively engaged in pursuing more telemetry and spacecraft operational information. We are interested in telemetry from orbits other than in GEO. We are in the progress of getting access to Van Allen Probes data, Lunar Reconnaissance Orbiter (LRO) data, and data from Air Force Research Laboratory (AFRL) spacecraft. These spacecraft are selected because each is equipped with dedicated space environment

monitoring technology, which will allow for better validation of algorithms. Events that are detected in the telemetry can be directly compared to the local space weather environment as detected on-board. The data providers have also indicated that they would be able to supply command logs and other operational information.

As mentioned before, we will also be investigating different data resolutions and will work on acquiring spacecraft operational commanding information. We will work on determining if there is a certain resolution that is the lower limit for the detection of certain types of events.

The amplifier system (roughly half of the telemetry analyzed in this thesis) may be less sensitive to the space weather environment due to its location deep within the spacecraft structure (*i.e.,* more shielded from the space environment than other components). We would expect to find that certain components are more or less sensitive to external space environment effects, either by their location within the spacecraft or their design and function (*e.g.,* a magnetometer). Therefore, we plan to obtain larger datasets that are representative of the entire spacecraft. For example, a dataset could include magnetometer data, thruster data, power system data, etc. Accompanying spacecraft operational information, such as maneuvers and commanded changes, will be imperative to evaluating possible internal effects on the telemetry that might be identified by the algorithms.

### Algorithm Development

For algorithm development, we plan to add in methods to detect larger-scale (longer-term, seasonal or yearly) and other unusual features and trends in the telemetry, such as changes in the slope of the local data or changes in the noise envelope (or variance). The scale of the longer-term changes will be defined using techniques such as principal component analysis and clustering of similar structures. The resulting information will enable variable bin sizing that is could be more appropriate for the scale of the changes. The statistics for each bin can be used to detect changes in the slope of the data and the change in the amount of noise in the data.

The current algorithms are retrospective, "batch" algorithms, looking back at pre-

vious windows of data and analyzing them. For eventual use in operations, we plan to enable real-time (or near-real-time) detection, moving the algorithms "online." This will require increasing the computational speed of the algorithms.

We plan to integrate learning algorithms for use after a certain period of time on orbit. While we do not want to rely on it for early operations or for changing or new environments, learning could be beneficial once in a nominal orbit, such as once in Martian orbit. The training does not have to be in advance or real-time. We are looking into techniques that, after a certain amount of elapsed mission time, can use learning by modeling previously seen telemetry. The response to hazards using the initially proposed algorithms can be fast, but the learning can be slow, supplementing algorithms if there are nominal operating periods.

Future work also includes sensor fusion techniques to intelligently combine the results from different event detection methods, transient event detection and change point event detection. Based on a preliminary assessment, we plan to use the JDL (Joint Directors of Laboratories) data fusion framework [142]. We will make a "situation assessment" (level 2); this assessment aims to identify the most likely situations given the observed events and trends [142]. It establishes relationships between the sensors of interest, determining the significance of the relationships. The determination of relationship significance, in this case, is informed by the findings from the telemetry response in certain scenarios (both internally and externally).

From learning, intelligent weighting can be incorporated to yield a spacecraft system health state estimation. For health state estimation techniques, we are considering Kalman filters and maximum a posteriori (MAP) techniques [25]. An extension of this work can be to take it to an "impact assessment": projecting the possible outcomes (risks, vulnerabilities, and opportunities) with prediction and estimation techniques [142]. These techniques can be integrated with autonomous software for on-board decision-making.

Informed by analysis of previous mission data, we plan to incorporate diagnosis into the algorithms. This will inform on-board decision making algorithms of how to react or which action to take (since the source of the event will be provided with

a confidence interval). We are considering model-based techniques, such as analytical models, which compute the residuals between measured and estimated variables. Fault diagnosis is achieved by (1) residual generation, (2) residual evaluation, (3) application of the appropriate decision logic [54]. There are also model-based methods that rely on physical models and Bayesian networks, which we will likely not consider based on the dependence on specific components and computational requirements, respectively.

The confidence in the algorithm findings can be determined by integrating statistical testing methods. We plan to incorporate an associated statistical significance with each event detected in the next iteration of the algorithms by implementing hypothesis testing (*i.e.,* null hypothesis is that there is no change in the distribution/data) and Monte Carlo simulations.)

### 5.3.2 Future Applications and Impacts

The implications of the development of these algorithms are far-reaching for future satellites. Applications can be found in the interest in in-orbit servicing, many satellite constellations, and deep space missions.

There is an interest in the ability to service satellites in-orbit, especially in contested orbits such as GEO. The interest is echoed in many recent solicitations, including a DARPA Request for Information in 2014. The algorithm suite could enable greater space situational awareness for the servicing satellites, to have an in-situ measurement of the local environment. The algorithms also help the satellite needing servicing by allowing detection and diagnosis of unusual performance or behavior.

In recent years, enabled by lower costs of small satellites and greater launch opportunities, several companies have proposed constellations of hundreds of small satellites (*e.g.,* LEOsat, OneWeb, SpaceX). Constellations provide data and media distribution services as well as imaging and weather observations. As our society increases its dependence on satellite services for comm and navigation, there is a growing need for efficient systems monitoring and space situational awareness to avoid service interruptions due to hazards such as space weather and orbital debris. Long time major

spacecraft operator players operate tens of satellites at once. Shifting to operating hundreds of satellites necessitates a change in the role of satellite and operator. Reduced dependence on ground control is a must, which includes the ability to identify and react to hazards autonomously on-board.

# Appendix A

# The Space Radiation Environment

The three principal sources of radiation to be considered are those emanating from the Sun, trapped particles in Earth's magnetic field, and Galactic Cosmic Rays. Solar variability drives the strength and frequency of Solar Particle Events and the Earth's magnetosphere strongly influences the sources of radiation by shielding the Earth (and near-Earth orbiting satellites) from hazardous levels of energetic particles.

## A.1 Solar Environment

The Sun dominates the solar system environment, with a mass of nearly $2\times10^{30}$ kg (99.9% of the total mass of the solar system) and a radius of $\sim7\times10^{8}$ km. The Sun is classified as a G2V main sequence star, emulating a black body with peak emissions at around 460 nm (giving the Sun a yellowish appearance). Solar emissions include electromagnetic (EM) radiation, a constant solar wind, and Solar Energetic Particles (SEPs). The magnitude and frequency of eruptive and particle events from the Sun are mostly dominated by the solar cycle.

### Solar Emissions

Electromagnetic (EM) radiation via continuous photons provides all heat and light input to the solar system. The Sun has an average luminosity of $3.85\times10^{26}$ W, the

brightness of which decreases as the inverse of the square of the object's distance from the Sun ($\sim 1/r^2$). At Earth, the solar radiation per unit area (the "solar constant") is roughly 1361 W/m$^2$ [70] and takes approximately 8 minutes to arrive at 1 Astronomical Unit (AU) ($\sim 1.496 \times 10^8$ km). The EM radiation is in the radio, visible, ultraviolet (UV), and X-ray wavelengths.

In addition to EM radiation, the Sun continuously ejects matter into space [84]. This stream of energized charged particles is called the "solar wind." The huge bubble of supersonic plasma is primarily composed of electrons and protons thermally-driven outward from the Sun. The magnetic field of the plasma has variable direction, with an average strength of around 5 nT. The solar wind varies in temperature, speed, and density. The solar wind temperature is around $10^5$ to $10^6$ K and the speed is about 400 km/s (~3-4 days to reach Earth), but can be boosted by coronal holes. The density of the solar wind when it reaches Earth's magnetosphere (discussed further in Section A.2) is about 9 protons/cm$^2$ [42].

Solar energetic particles (SEPs) are protons, electrons, and heavier nuclei that are 10s of MeV to GeV. These particles are intermittent and bursty and can arrive at Earth within a few hours, or as short as 15 minutes. Eruptive events and solar particle events are discussed in further detail in this section.

## Solar Variability

The Sun is a variable source, significantly impacting the solar environment. The "solar cycle" is ~11 years, with a full cycle lasting ~22 years. The cycle cause is believed to be related to the reversal of the Sun's magnetic field, which reverses every eleven years and makes a full cycle (returning to the original polarity) after about 22 years. Fueled by the solar dynamo, increased magnetic variability in the Sun causes flux emergences, such as sunspots, coronal loops, and other phenomena, which are the manifestations of magnetic flux tubes that form in the solar interior and pass through the solar surface.

Sunspots (or, more generally, bipolar active regions) are conduits for the transport of magnetic energy and flux from the solar interior to the solar corona. As such,

sunspots are an indication that there are significant disturbances in the magnetic field lines on the Sun's surface and through its atmosphere. Sunspots appear as dark spots (due to the spot being cooler than the surrounding surface) and were first observed in the 1600s by Galileo. The solar cycle strength is defined by the Wolf Zurich sunspot number[1], which is used to quantify the overall number of sunspots on the Sun at any time. Figure A-1 shows the number of sunspots during the previous and most recent solar cycles (solar cycles 23 and 24).

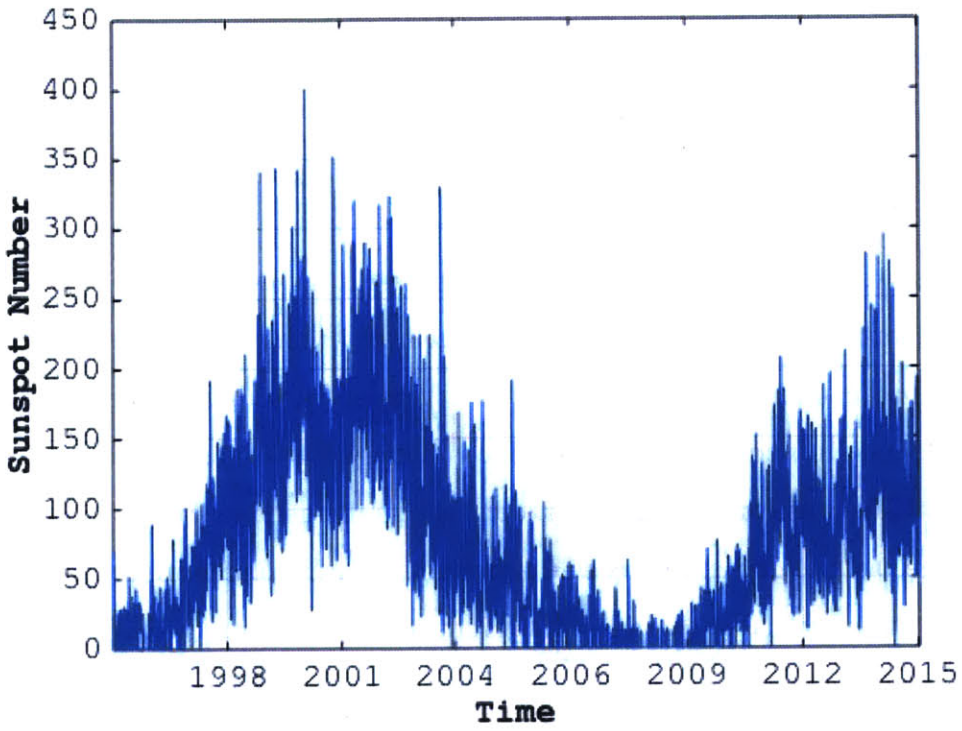


Figure A-1: Sunspot numbers as a function of time from Solar Cycles 23 and 24 (ongoing). Solar cycle 24 began in January 2008. Sunspot data from SILSO Data Files, Royal Observatory of Belgium, Brussels [147].

The solar cycle has a large impact on the solar system environment, regulating nearly all solar variability in irradiance, solar wind, flares, coronal mass ejections,

[1]The sunspot number calculation by NOAA SWPC is in the process of a revision. The calibration factor applied for over one hundred years appears to be inaccurate, so the factor is being removed. This will reconcile discrepancies between the two major sunspot number reporting forms (the other being the Group Number). The full transition by NOAA SWPC will take place in the solar minimum between cycles 24 and 25. Initial findings indicate better correlation between space weather indices and the revised sunspot number [31]. See Clette et al. (2014) for a detailed explanation and findings.

etc. Solar maximum is characterized by increased radiation emissions in radio, X-ray, and gamma-ray energies. Solar particle events (SPEs), solar flares, and coronal mass ejections (CMEs) are much more frequent and likely during periods of solar maximum, occurring at frequencies of up to every few hours, lasting from a few minutes to several hours [53].

## Solar Particle Events (SPEs)

Eruptive events originating from the Sun are powered by an explosive conversion of magnetic energy into radiative or kinetic energy, producing solar flares or coronal mass ejections (CMEs), respectively. Solar flares and CMEs can cause strong interplanetary shock waves, which can lead to geomagnetic storm activity and magnetosphere coupling [22, 53].

Solar flares are a sudden burst of radiation lasting minutes or hours. Solar flares are associated mainly with X-ray radiation, but other radiation is also present at wavelengths that can include hard X-rays and gamma-rays (via Bremsstrahlung), soft (thermal) X-rays and EUV (multi-million degree Kelvin gas), hydrogen-alpha (hot chromosphere emissions), and GHz radio bursts (energetic electrons in magnetic fields). A large quantity of energy is released from a small volume in a short period of time. Since the only viable energy source is intense solar magnetic fields, the flares must be fueled by a very rapid means of converting stored magnetic energy into a particle energy and heat, *i.e.,* magnetic reconnection. For more details on magnetic reconnection, see "Magnetic Reconnections" by Priest and Forbes (2000) [102].

Coronal mass ejections (CMEs) are huge bubbles of plasma ejected from the Sun. The most distinguishing feature of a CME is a strong magnetic field with large out-of-the-ecliptic components. The ejection speed can be anywhere from 10s of km/s to 2000 km/s, making an Earth arrival in 24 to 36 hours or as short as 14 to 17 hours. CME formation models involve the release of plasma being held down by closed magnetic loops via magnetic reconnection. The magnetic fields are stressed through the motion of the photospheric footprints. Once released, the magnetic buoyancy forces quickly accelerate the plasma away from the Sun [102].

Co-rotating Interaction Regions (CIRs) form in response to fast solar wind interacting with slower solar wind, generally recurring every 27 days (~1 solar revolution on its spin axis) [132]. CIRs cause fluctuations in the solar wind, particularly in the $B_z$ component of the interplanetary magnetic field (IMF) and are effective at causing strong increases in high-energy electrons in the outer radiation belt [73, 86]. It is possible for the relativistic electrons of a CIR to produce higher levels of deep dielectric charging than CMEs [21].

Solar energetic particles (SEPs) originate from magnetic reconnection and shock acceleration. Both flares and CMEs can generate shocks in the corona, and fast CMEs can generate shocks in the solar wind. Both flares and CMES are powered by the release of magnetic energy in the Sun's corona through magnetic reconnection. Part of the energy in these events is in the form of nuclei accelerated to high energies and released into space. As described previously for CMEs, the particle types are protons, electrons, and some heavier nuclei. The particle energies can range from a few tens of keV to GeV (the fast particles can reach 80% of the speed of light). Proton and electron events are the most commonly measured, as they can have a large impact of spacecraft and life, especially when energies above ~1 MeV for protons and ~20 MeV for electrons are reached (see Figure 1-2). SEPs travel easily along magnetic fields (they can also scatter (diffuse) across field lines, but more slowly). SEPs arrive promptly at Earth when the Earth is connected magnetically to the source region.

Commonly used metrics to describe solar particle events, in addition to the energies, are flux and fluence. Both the peak flux of an event and the build up of flux over time (fluence) can have detrimental effects on a satellite (*e.g.*, [71, 78, 89]). Flux is the rate at which particles flow through a given area. Flux typically has units of particles/cm$^2$ s$^1$ sr$^1$. Flux is commonly quoted with respect to a given energy. Differential flux is the flux at a certain energy and integral flux, as the name implies, is the integrated flux at a certain energy and higher. Fluence $F$ is the accumulation of flux $J$ over time $T$: $F(T) = \int_0^T J(t)dt$. Fluence at a given energy typically has units of particles/cm$^2$. Another commonly used metric is total ionizing dose (TID), which is the total energy per unit mass of material transferred to the material via ionization

from all ionizing radiation [99, 124]. This metric is dependent on the specifics of the satellite (*e.g.*, shielding, materials). The energy delivered, and therefore the exact nature of the potential damage incurred, is dependent on the particle type.

## A.2 Near-Earth Environment

A second radiation hazard is the trapped energetic particle environment in Earth's magnetic field, known as the Van Allen radiation belts. The belts differ in distribution and energy for protons and electrons. They are generally located at about 1 $R_E$ to 4 $R_E$ with energies of about 0.1 - 400 MeV and at about 2 $R_E$ to 8 $R_E$ with energies of about 0.4 - 4.5 MeV for protons and electrons, respectively [53]. Figure A-2 shows the distribution of particles as a function of altitude.

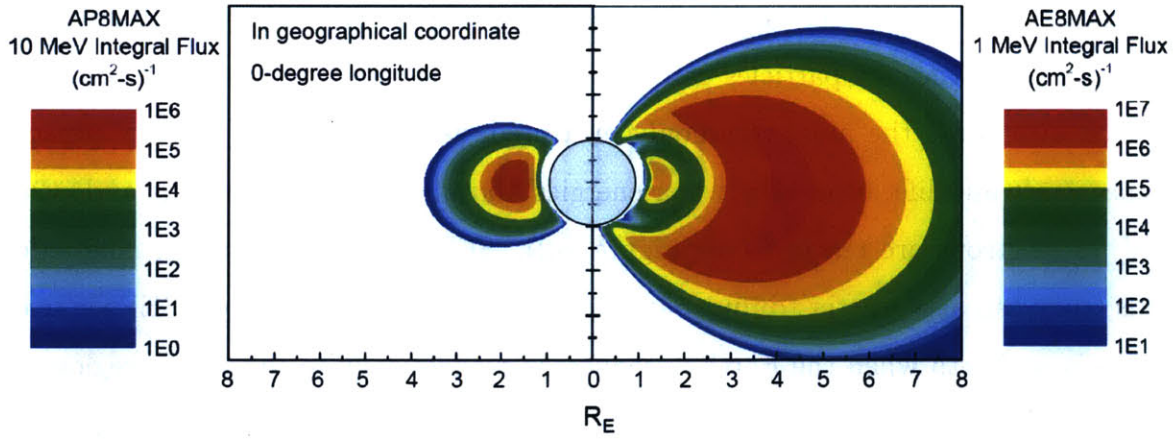


Figure A-2: Distribution of protons and electrons as a function of altitude and energy in Earth orbit at zero degrees longitude, using the AP8/AE8 models at solar maximum.

While the trapped radiation belts provide protection from the direct effects of solar storms to regions inside the belts, they are a hostile environment to satellites located within or passing through the belts [22]. Many satellite operational anomalies are reported from within the belts [9, 22], so the belt orbits are often avoided if possible.

The AE8 and AP8 models (and now AE9/AP9 models) are typically used to predict the variations in the belts [50, 111, 134]. However, the variations are still not

well understood and the focus of current research efforts [105]. To better understand and characterize the radiation belt environments, the Van Allen Probes (two satellites supported by NASA's Heliophysics division "Living With a Star" program) are dedicated space environment monitoring of the radiation belts, revealing unprecedented details on the belts and working on determining the physical mechanisms leading to their formation, sustained existence, and their variability [11].

A disturbance in the belts that is particularly well-characterized (due to the number of satellites that experience it) is the South Atlantic Anomaly. Satellites in LEO see a variation in radiation flux as they pass through their orbits. The SAA is a region of higher radiation caused by the difference in alignment of Earth's rotational and magnetic axes, causing the inner belt to be closer to the Earth over the South Atlantic [22]. The SAA is taken into account in the design and operation any LEO satellite that will pass through it, as the increased radiation can have a large impact on the satellite [53]. It should be noted that the SAA is not static; it moves in response to Earth's changing magnetic field.

## A.3 Galactic Environment

Galactic cosmic rays (GCRs) are particles produced by high-energy events (such as the acceleration processes from supernova events), which travel at relativistic speeds. The types of particles and masses are varied: from a single proton up to higher atomic number nuclei. GCRs are predominantly protons (~83% hydrogen), with contributions from alpha particles (~15% helium), few electrons, and less than 1% heavier nuclei [9, 42, 114, 143]. GCRs have energies up to $10^{14}$ MeV [22] and typically occur out of phase with the solar cycle; radiation from GCRs peaks at the declining phase of the solar cycle and solar minimum and reaches a minimum at solar maximum. At solar minimum, the solar wind speeds and densities are low, allowing GCRs to reach the magnetosphere [53, 107].

The Cosmic Ray Telescope for the Effects of Radiation (CRaTER) instrument on the Lunar Reconnaissance Orbiter (LRO) measures solar energetic protons and

galactic cosmic rays in lunar orbit (particularly ions with energies greater than 10 MeV) [123]. Analysis of CRaTER measurements has confirmed the weak modulation of GCRs in the past 25 years due to low interplanetary magnetic fields and prolonged periods of little solar activity [113].

Cosmic rays have free access to the near-Earth environment, particularly over the polar regions where the magnetic field lines are open to interplanetary space. Satellites in high inclination orbits such as sun synchronous orbit are exposed to higher radiation from GCRs moving along Earth's magnetic field lines, which converge at the magnetic poles [15]. While the flux rate is low, GCRs can produce intense ionization as they pass through matter due to their relativistic speeds and high energies. The extreme energies and relative unpredictability of GCRs pose a threat to spacecraft. A GCR loses energy mainly by ionization, where the energy loss is dependent on the square of the particle's charge, $Z$, which can be increased if the particle undergoes nuclear interactions within the electronic part. Therefore, lower $Z$ ions (which are more abundant) deposit as much energy as less abundant, higher $Z$ ions [141].

In addition to particles, intense amounts of gamma radiation perforate the galaxy [22]. For the most part, the Earth's magnetic field provides shielding for spacecraft from galactic radiation, so this is likely not a concern for most spacecraft.

# Appendix B

# Event Analysis

| Event Data Analysis | Space Weather | | | | Other Reported Anomalies | Known Spacecraft Events | |
|---|---|---|---|---|---|---|---|
| Event Date | GOES >2 MeV Electrons (daily fluence, particles/cm2) | GOES >10 MeV Protons (daily fluence, particles/cm2) | Kp Index | CMEs, Interplanetary CMEs, comments | Known satellite anomalies | Operations/Maneuvers | SEUs/SSC w/in 1 week of Event Dat |
| 3-Dec-08 | quiet, 3.3e6 | quiet, 1.9e4 | quiet, kp=1 | none | GOES 12 thruster problems 12-Dec-2008 | | Transponder SEU Dec 2008 |
| 9-Sep-04 | relatively quiet, 4.7e7 | quiet, 1.4e4 | quiet, kp=0 | coronal hole spewing solar wind, to arrive at Earth 6-7 Sep 2004 | Thaicom 3 outages for several hours 12-Sep-2004 | | SEU Sep 12, 2004 |
| 28-Oct-13 | relatively quiet, 2.1e7 | relatively quiet, 1.7e5 | quiet, kp=0 | Handful of powerful CMEs starting Oct. 25, several associated X-class flares | | | |
| 30-Jul-13 | relatively quiet, 3.2e7 | quiet, 1.1e4 | quiet, kp=1 | peak of southern Delta Aquariid meteor shower, pair of CMEs 26-Jul-2013, but not really Earth-directed, glancing | | | |
| 4-Nov-97 | quiet, 1.2e7 | relatively quiet, 1.8e6 | quiet, kp=2 | | | Maneuver between 1-13 Nov 1997 | |
| 2-Jul-99 | quiet, 4.7e6 | quiet, 1.5e4 | moderate, kp=4 | | Echostar IV fuel system anomalies July 1999, ABRIXAS failure of onboard batteries | | |
| 28-Feb-10 | quiet, 6.1e5 | quiet, 1.9e4 | quiet, kp=0 | 28-Feb-2010 large CME, not Earth-directed | AMC-16 further degradation of solar arrays early March 2010, GEO | Maneuver between 23 Feb to 07 Mar 2010 | Transponder SEU Feb 27, 2010 |

# Bibliography


[1] Richard Abbot and Timothy Wallace. Decision Support in Space Situational Awareness. *MIT Lincoln Laboratory Journal*, 16(2), 2007.

[2] Bovas Abraham and George E. P. Box. Bayesian Analysis of Some Outlier Problems in Time Series. *Biometrika*, 66:229–236, August 1979. doi:10.2307/2335653.

[3] Bovas Abraham and Alice Chuang. Outlier Detection and Time Series Modeling. *Technometrics*, 31:241–248, May 1989. doi:10.2307/1268821.

[4] Advanced Composite Explorer (ACE) Science Center. New ACE Level 2 Data Server. Accessed: August 2015. URL: http://www.srl.caltech.edu/ACE/ASC/level2/new/intro.html.

[5] Rakesh Agrawal and Ramakrishnan Srikant. Mining Sequential Patterns. In *Proceedings of the 11th International Conference on Data Engineering*, pages 3–14, Taipei, March 1995. IEEE. doi:10.1109/ICDE.1995.380415.

[6] Joe Allen and William F. Denig. Satellite Anomalies, 1993. URL: http://www.ngdc.noaa.gov/stp/satellite/anomaly/satelliteanomaly.html /doc/anomalies.txt.

[7] Joe Allen and William F. Denig. Summary Report, Spacecraft Anomaly Data, 1997. URL: http://www.ngdc.noaa.gov/stp/satellite/anomaly/doc/5jsumm.txt.

[8] Frank J. Anscombe and Irwin Guttman. Rejection of Outliers. *Technometrics*, 2(2):123–147, May 1960. doi:10.2307/1266540.

[9] Daniel N. Baker. The Occurrence of Operational Anomalies in Spacecraft and Their Relationship to Space Weather. *IEEE Transactions on Plasma Science*, 28(6), 2000. doi:10.1109/27.902228.

[10] Daniel N. Baker. How to Cope with Space Weather. *Science*, 297:1486–1487, 2002. doi: 10.1126/science.1074956.

[11] Daniel N. Baker, S. G. Kanekal, V. C. Hoxie, S. Batiste, M. Bolton, X. Li, S. R. Elkington, S. Monk, R. Reukauf, S. Steg, J. Westfall, C. Belting, B. Bolton,

D. Braun, B. Cervelli, K. Hubbell, M. Kien, S. Knappmiller, S. Wade, B. Lamprecht, K. Stevens, J. Wallace, A. Yehle, H. E. Spence, and R. Friedel. The Relativistic Electron-Proton Telescope (REPT) Instrument on Board the Radiation Belt Storm Probes (RBSP) Spacecraft: Characterization of Earth's Radiation Belt High-Energy Particle Populations. *Space Science Reviews*, 179(1):337–381, 2012.

[12] Sabyasachi Basu and Martin Meckesheimer. Automatic Outlier Detection for Time Series: An Application to Sensor Data. *Knowledge and Information Systems*, 11(2):137–154, August 2007. doi:10.1007/s10115-006-0026-6.

[13] Sugato Basu, Mikhail Bilenko, and Raymond J. Mooney. A Probabilistic Framework for Semi-Supervised Clustering. In *Proceedings of the 10th ACM SIGKDD International Conference on Knowledge Discovery and Data Mining*, pages 59–68. ACM Press, 2004. doi:10.1145/1014052.1014062.

[14] Bryan L. Benedict. Investing in Satellite Life Extension - Fleet Planning Options for Spacecraft Owner/Operators. In *AIAA SPACE 2014 Conference and Exposition*, San Diego, CA, 2014. AIAA. doi:10.2514/6.2014-4445.

[15] Eric R. Benton and E.V Benton. Space Radiation Dosimetry in Low-Earth Orbit and Beyond. *Nuclear Instruments and Methods in Physics Research Section B: Beam Interactions with Materials and Atoms*, 184(1–2):255–294, 2001.

[16] Ruchita Bhargava, Hillol Kargupta, and Michael Powers. Energy Consumption in Data Analysis for On-board and Distributed Applications. In *Applications, Proceedings of the ICML'03 workshop on Machine Learning Technologies for Autonomous Space Applications*, volume 3, 2003.

[17] Ana Maria Bianco, Marta Garcia Ben, E. J. Martinez, and Victor J. Yohai. Outlier Detection in Regression Models with ARIMA Errors using Robust Estimates. *Journal of Forecasting*, 20:565–579, December 2001. doi:10.1002/for.768.

[18] Michael J. Bodeau. High Energy Electron Climatology that Supports Deep Charging Risk Assessment in GEO. In *48th AIAA Aerospace Sciences Meeting Including the New Horizons Forum and Aerospace Exposition*, Orlando, FL, May 2010. American Institute of Aeronautics and Astronautics. doi:10.2514/6.2010-1608.

[19] Boeing. GOES N Databook. Technical Report CDRL PM-1-1-03 Rev D, Contract NAS5-98069, National Aeronautics and Space Administration, Goddard Space Flight Center, Greenbelt, MD, November 2009.

[20] Alexander Bogorad, C. Bowman, A. Dennis, J. Beck, D. Lang, and Roman Herschitz. Integrated Environmental Monitoring System for Spacecraft. *IEEE Transactions On Nuclear Science*, 42(6):2051–2057, 1995. doi:10.1109/23.489252.

[21] Joseph E. Borovsky and Michael H. Denton. Differences Between CME-driven Storms and CIR-driven Storms. *Journal of Geophysical Research: Space Physics*, 111(A7), 2006. A07S08.

[22] Volker Bothmer and Ioannis Daglis. *Space Weather: Physics and Effects.* Springer-Verlag Berlin Heidelberg, 2007. doi:10.1007/978-3-540-34578-7.

[23] Christopher Bowman and Duane DeSieno. Detecting, Classifying, and Tracking Abnormal Data in a Data Stream. US Patent: US8306931, B1, November 2012.

[24] W.L. Brown and J.D. Gabbe. The Electron Distribution in the Earth's Radiation Belts during July 1962 as Measured by Telstar. *Journal of Geophysical Research*, 68(3):607–618, March 1963. doi:10.1029/JZ068i003p00607.

[25] James V. Candy. *Bayesian Signal Processing: Classical, Modern and Particle Filtering Methods.* John Wiley & Sons, April 2011. ISBN: 978-0-470-18094-5.

[26] Ashley K. Carlton. Towards a Viable Satellite Anomaly Database for GEO Communications Satellites. Final paper for MIT 22.16 Nuclear Technology and Society, May 2015.

[27] Varun Chandola, Arindam Banerjee, and Vipin Kumar. Anomaly Detection: A Survey. *ACM Computing Surveys*, 41(3):1–72, July 2009. Article 15.

[28] Da Chen, Xueguang Shao, Bin Hu, and Qingde Su. Simultaneous Wavelength Selection and Outlier Detection in Multivariate Regression of Near-Infrared Spectra. *Analytical Sciences*, 21:161–166, February 2005. doi:10.2116/analsci.21.161.

[29] Dakai Chen, James D. Forney, Ronald L. Pease, Anthony M. Phan, Martin A. Carts, Stephen R. Cox, Kirby Kruckmeyer, Sam Burns, Rafi Albarian, Bruce Holcombe, Bradley Little, James Salzman, Geraldine Chaumont, Herve Duperray, Al Ouellet, and Kenneth LaBel. The Effects of ELDRS at Ultra-Low Dose Rates. In *IEEE Radiation Effects Data Workshop*, Denver, CO, July 2010. doi:10.1109/REDW.2010.5619506.

[30] Mooi Choo Chuah and Fen Fu. ECG Anomaly Detection via Time Series Analysis. In *Frontiers of High Performance Computing and Networking ISPA 2007 Workshops*, pages 123–135. Springer, 2007.

[31] Frederic Clette, Leif Svalgaard, Jose. M. Vaquero, and Edward W. Cliver. Revisiting the Sunspot Number. A 400-Year Perspective on the Solar Cycle. *Space Science Reviews*, 186:35–103, December 2014. doi:10.1007/s11214-014-0074-2.

[32] E.J. Daly, A. Hilgers, G. Drolshagen, and Hugh Evans. Space Environment Analysis: Experience and Trends. In *Environment Modelling for Space-based Applications, Symposium Proceedings (ESA SP-392)*, Noordwijk, The Netherlands, September 1996. 10.1007/978-94-015-9395-3.

[33] Dorothy E. Denning. An Intrusion Detection Model. *IEEE Transactions on Software Engineering*, SE-13:222–232, February 1987. doi:10.1109/TSE.1987.232894.

[34] Richard O. Duda, Peter E. Hart, and David G. Stork. *Pattern Classification.* John Wiley & Sons, Second edition, 2001.

[35] Eleazar Eskin. Anomaly Detection over Noisy Data using Learned Probability Distributions. In *Proceedings of the 17th International Conference on Machine Learning*, pages 255–262. Morgan Kaufmann Publishers, Inc., 2000.

[36] Eleazar Eskin, Wenke Lee, and Salvatore J. Stolfo. Modeling System Call for Intrusion Detection using Dynamic Window Sizes. In *Proceedings of DARPA Information Survivability Conference and Exposition (DISCEX)*, volume 1, pages 165–175, Anaheim, CA, 2001. doi:10.1109/DISCEX.2001.932213.

[37] Philippe Esling and Carlos Agon. Time-Series Data Mining. *ACM Computing Surveys*, 45(1), November 2012. Article 12, doi:10.1145/2379776.2379788.

[38] European Space Agency. Space Situational Awareness Programme Overview. Accessed December 2015. http://www.esa.int/Our_Activities/Operations/Space_Situational_Awareness/SSA_Programme_overview.

[39] Tom Fawcett and Foster Provost. Activity Monitoring: Noticing Interesting Changes in Behavior. In *Proceedings of the 5th ACM SIGKDD International Conference on Knowledge Discovery and Data Mining*, pages 53–62, San Diego, CA, August 1999. ACM Press. doi:10.1145/312129.312195.

[40] Joseph Fennell, H.C. Koons, Jim Roeder, and J.B. Blake. Spacecraft Charging: Observations and Relationships to Satellite Anomalies. Aerospace Report tr-2001(8570)-5, Aerospace Corporation, El Segundo, CA, 2001.

[41] Dale Ferguson and G.B. Hillard. Low Earth Orbit Spacecraft Charging Design Guidelines. Technical Report TP 2003 212287, National Aeronautics and Space Administration, 2003.

[42] Peter Fortescue, Graham Swinerd, and John Stark. *Spacecraft Systems Engineering.* John Wiley & Sons, Ltd., West Sussex, UK, fourth edition, 2011.

[43] Jeff Foust. The Return of the Satellite Constellations. Accessed: Dec 2015. URL: http://www.thespacereview.com/article/2716/1.

[44] Arthur R. Frederickson. Upsets Related to Spacecraft Charging. *IEEE Transactions on Nuclear Science*, 23(2):426–441, April 1996. doi:10.1109/23.490891.

[45] Ryohei Fuijmaki, Takehisa Yairi, and Kazuo Machida. An Approach to Spacecraft Anomaly Detection Problem using Kernel Feature Space. In *Proceedings of the 11th ACM SIGKDD International Conference on Knowledge Discovery in Data Mining*, pages 401–410, Chicago, IL, 2005. KDD, ACM Press. doi:10.1145/1081870.1081917.

[46] David A. Galvan, Brett Hemenway, William Welser, and Dave Baiocchi. Satellite Anomalies: Benefits of a Centralized Anomaly Database and Methods for Securely Sharing Information Among Satellite Operators, 2014. The RAND Corporation.

[47] Joeseph Gangestad, Darren Rowen, Brian Hardy, Christopher Coffman, and Paul O'Brien (The Aerospace Corporation). Flight Results from AeroCube-6: A Radiation Dosimeter Mission in the 0.5U Form Factor. In *CubeSat Developers' Workshop*, San Luis Obispo, CA, April 2015.

[48] Henry Garrett and Albert Whittlesey. *Guide to Mitigating Spacecraft Charging Effects.* JPL Space Science and Technology Series. John Wiley & Sons, Inc., Pasadena, CA, May 2012.

[49] William H. Gerstenmaier. NASA's Asteroid Redirect Mission. In *AIAA SPACE Conference and Exposition*, San Diego, CA, 2013.

[50] Greg Ginet, Paul O'Brien, S. Huston, W. Johnston, Timothy Guild, R. Friedel, C. Lidstrom, C. Roth, P. Whelan, R. Quinn, D. Madden, Steven Morley, and Yi Jiun Su. AE9, AP9 and SPM: New Models for Specifying the Trapped Energetic Particle and Space Plasma Environment. *Space Science Reviews*, 179:579–615, March 2013. doi:10.1007/s11214-013-9964-y.

[51] Andrea Guiotto, Andrea Martelli, and Carlo Paccagnini. SMART-FDIR: Use of Artificial Intelligence in the Implementation of a Satellite FDIR. In *Proceedings of DASIA: Data Systems in Aerospace (ESA SP-532)*, Prague, Czech Republic, June 2003. SAGE Publications. doi:10.1177/0954410011421717.

[52] Eric Hand. Startup Liftoff. *Science*, 348(6231), April 2015. DOI: 10.1126/science.348.6231.172.

[53] Daniel Hastings and Henry Garrett. *Spacecraft-Environment Interactions.* Cambridge Atmospheric and Space Science Series. Cambridge University Press, Cambridge, UK, 1996.

[54] David Henry, Silvio Simani, and Ron J. Patton. *Fault Tolerant Flight Control: Fault Detection and Diagnosis for Aeronautic and Aerospace Missions*, pages 91–128. Lecture Notes in Control and Information Sciences. Springer Verlag, Berlin, 2010.

[55] Wilmot N. Hess. The Effects of High Altitude Explosions. Technical Report TN D-2402, National Aeronautics and Space Administration, 1964.

[56] Hugh de Lacy and Alun Jones. Shrinking Silicon Feature Sizes: Consequences for Reliability. In *Conference for Military and Space Electronics (CSME)*, Portsmouth, UK, 2008.

[57] Inmarsat. About Us: Our Satellites, 2013. URL: http://www.inmarsat.com/about-us/our-satellites/.

[58] Intelsat. About Us: Overview, 2015. URL: http://www.intelsat.com/homepage/about-us/overview/.

[59] Minoru Inui, Yashinobu Kawahara, Kohei Goto, Takehisa Yairi, and Kazuo Machida. Adaptive Limit Checking for Spacecraft Telemetry Data Using Kernal Principal Component Analysis. In *Transactions of the Japan Society for Aeronautical and Space Sciences, Space Technology Japan*, volume 7, pages 11–16, Japan, December 2009.

[60] Space Operations Joint Chiefs of Staff. Joint Publication 3-14. http://www.dtic.mil/doctrine/new_pubs/jp3_14.pdf, May 2013.

[61] Ian T. Jolliffe. *Principal Component Analysis.* Springer-Verlang New York, Second edition, 2002. doi:10.1007/b98835.

[62] Michael J. Kearns. *Computational Complexity of Machine Learning.* MIT Press, 1990. Revision of doctoral dissertation, Harvard University, May 1989.

[63] Eamonn Keogh, Jessica Lin, Sang-Hee Lee, and Helga Van Herle. Finding the Most Unusual Time Series Subsequence: Algorithms and Applications. *Knowledge and Information Systems*, 11(1):1–27, January 2007. doi:10.1007/s10115-006-0034-6.

[64] Eamonn Keogh, Stefano Lonardi, and Bill 'Yuan chi' Chiu. Finding Surprising Patterns in a Time Series Database in Linear Time and Space. In *Proceedings of the 8th ACM SIGKDD International Conference on Knowledge Discovery and Data Mining*, pages 550–556, Edmonton, AB, July 2002. ACM Press. doi:10.1145/775047.775128.

[65] Eamonn J. Keogh, Selina Chu, David Hart, and Michael J. Pazzani. Segmenting Time Series: A Survey and Novel Approach. *Data Mining in Time Series Databases*, 57:1–22, 2004. doi: 10.1142/9789812565402_0001.

[66] Eamonn J. Keogh and Michael J. Pazzani. An Enhanced Representation of Time Series Which Allows Fast and Accurate Classification, Clustering, and Relevance Feedback. In *Proceedings of the 4th International Conference on Knowledge Discovery and Data Mining (KDD-98), AAAI Press*, pages 239–241, New York, NY, 1998.

[67] Daniel Kifer, Shai Ben-David, and Johannes Gehrke. Detecting Change in Data Streams. In *Proceedings of the 30th very Large Data Bases Conference*, volume 30, pages 180–191, Toronto, 2004.

[68] Peter C. Klanowski. About Sat-ND, Satellite News Digest. Accessed: May 2015. URL: http://www.sat-nd.com/info/about.php.

[69] Thanvarat Komviriyavut, Phurivit Sangkatsanee, Naruemon Wattanapongsakorn, and Chalermpol Charnsriprinyo. Network Intrusion Detection and Classification with Decision Tree and Rule Based Approaches. In *International Symposium on Communications and Information Technologies*, pages 1046–1050, Icheon, September 2009. IEEE. doi:10.1109/ISCIT.2009.5341005.

[70] Greg Kopp and Judith Lean. A New, Lower Value of Total Solar Irradiance: Evidence and Climate Significance. *Geophysical Research Letters*, 38(1), January 2011. doi:10.1029/2010GL045777.

[71] Shu T. Lai. *Fundamentals of Spacecraft Charging: Spacecraft Interactions with Space Plasmas.* Princeton University Press, Princeton, NJ, 2012.

[72] Lexiang Le, Xiaoyue Wang, Eamonn J. Keogh, and Agenor Mafra-neto. Autocannibalistic and Anyspace Indexing Algorithms with Applications to Sensor Data Mining. In *Proceedings of the SIAM International Conference on Data Mining*, pages 85–96, 2009.

[73] Xinlin Li, Daniel Baker, Michael Temerin, Geoffrey Reeves, Reiner Friedel, and Chuqiao Shen. Energetic Electrons, 50 keV to 6 MeV, at Geosynchronous Orbit: Their Responses to Solar Wind Variations. *Space Weather*, 3(4), March 2005. doi:10.1029/2004SW000105.

[74] Jessica Lin, Eamonn Keough, Ada Fu, and Helga Van Herle. Approximations to Magic: Finding Unusual Medical Time Series. In *Proceedings of the 18th IEEE Symposium on Computer-Based Medical Systems*, pages 329–334. IEEE, June 2005. doi:10.1109/CBMS.2005.34.

[75] Whitney Lohmeyer. Data Management of Geostationary Communication Satellite Telemetry and Correlation to Space Weather Observations. Master's thesis, Massachusetts Institute of Technology, Department of Aeronautics and Astronautics, February 2013.

[76] Whitney Lohmeyer. *Space Radiation Environment Impacts on High Power Amplifiers and Solar Cells On-board Geostationary Communications Satellites.* PhD dissertation, Massachusetts Institute of Technology, Department of Aeronautics and Astronautics, March 2015.

[77] Whitney Lohmeyer, Kerri Cahoy, and Daniel Baker. Correlation of GEO Communications Satellite Anomalies and Space Weather Phenomena: Improved Satellite Performance and Risk Mitigation. In *30th AIAA International Communications Satellite System Conference (ICSSC)*, Ottawa, Canada, 2012. doi:10.2514/6.2012-15083.

[78] Whitney Lohmeyer, Ashley Carlton, Frankie Wong, Michael Bodeau, Andrew Kennedy, and Kerri Cahoy. Response of Geostationary Communications Satellite Solid-State Power Amplifiers to High-Energy Electron Fluence. *AGU Space Weather*, 13(5):298–315, 2015. 2014SW001147.

[79] Markos Markou and Sameer Singh. Novelty Detection: A Review-Part 1: Statistical Approaches. *Signal Processing*, 83(12):2481–2497, December 2003. doi:10.1016/j.sigpro.2003.07.018.

[80] Markos Markou and Sameer Singh. Novelty Detection: A Review-Part 2: Neural Network Based Approaches. *Signal Processing*, 83(12):2499–2521, December 2003. doi:10.1016/j.sigpro.2003.07.019.

[81] Julien Marzat, Helene Piet-Lahanier, Frederic Damongeot, and Eric Walter. Model-Based Fault Diagnosis for Aerospace Systems: A Survey. In *Proceedings of the Institution of Mechanical Engineers, Part G: Journal of Aerospace Engineering*, volume 226, pages 1329–1360. SAGE Publications, 2012. doi:10.1177/0954410011421717.

[82] F. J. Massey. The Kolmogorov-Smirnov Test for Goodness of Fit. *Journal of the American Statistical Association*, 46(253):68–78, 1951.

[83] Claudia Meitinger and Axel Schulte. *Human-UAV Co-operation Based on Artificial Cognition*, volume 5639 of *Lecture Notes in Computer Science*, pages 91–100. Springer Verlag, Berlin, 2009.

[84] Nicole Meyer-Vernet. *Basics of the Solar Winds*. Cambridge University Press, Cambridge, UK, 2007. http://dx.doi.org/10.1017/CBO9780511535765.

[85] Jiun-Jih Miau and Richard Holdaway. Reducing the Cost of Spacecraft Ground Systems and Operations. In *Space Technology Proceedings*, volume 3. Springer Netherlands, 2000. 10.1007/978-94-015-9395-3.

[86] Yoshizumi Miyoshi and Ryuho Kataoka. Flux Enhancement of the Outer Radiation Belt Electrons after the Arrival of Stream Interaction Regions. *Journal of Geophysical Research: Space Physics*, 113, January 2008. doi:10.1029/2007JA012506.

[87] Paula Morgan. Fault Protection Techniques in JPL Spacecraft. In *Proceedings of the First International Forum on Integrated System Health Engineering and Management in Aerospace (ISHEM)*, Napa, CA, November 2005.

[88] R. China Appala Naidu and P. S. Avadhani. A Comparison of Data Mining Techniques for Intrusion Detection. In *Proceedings of IEEE International Conference on Advanced Communication Control and Computing Technologies (ICACCCT)*, pages 41–44, Ramanathapuram, August 2012. IEEE. doi:10.1109/ICACCCT.2012.6320731.

[89] National Aeronautics and Space Administration. Mitigating In-Space Charging Effect: A Guideline. Technical Report NASA HDBK 4002A, 2009.

[90] National Aeronautics and Space Administration. *NASA Strategic Plan.* Washington, D.C., 2014. NP-2014-01-964-HQ.

[91] National Oceanic and Atmospheric Adminsitration, Office of Science and Product Operations. GOES Operational Status. Accessed Jan. 19, 2016. http://www.ospo.noaa.gov/Operations/GOES/status.html.

[92] National Oceanic Atmospheric Administration. National Oceanic Atmospheric Administration National Weather Service Space Weather Prediction Center. Accessed: August 2015. URL: http://www.swpc.noaa.gov/.

[93] National Oceanic Atmospheric Administration National Geophysical Data Center. Access to GOES SEM Data. Accessed: August 2015. URL: http://www.ngdc.noaa.gov/stp/satellite/goes/dataaccess.html.

[94] National Resource Council. Severe Space Weather Events - Understanding Societal and Economic Impacts Workshop. Technical report, National Academy of Sciences, 2008. URL: http://www.nap.eduicatalog/12507.html.

[95] Paul O'Brien, Joseph E. Mazur, and Timothy B. Guild. Recommendations for Contents of Anomaly Database for Correlation with Space Weather Phenomena. Technical Report TOR-2011(3903)-5, The Aerospace Corporation, El Segundo, CA, 2011.

[96] Office of the Federal Coordinator for Meteorological Services and Supporting Research. Report on Space Weather Observing Systems: Current Capabilities and Requirements for the Next Decade. Technical report, Washington, D.C., 2013.

[97] Lucas Parra, Gustavo Deco, and Stefan Miesbach. Statistical Independence and Novelty Detection with Information Preserving Nonlinear Maps. *Neural Computation*, 8:260–269, February 1996. doi:10.1162/neco.1996.8.2.260.

[98] Emanuel Parzen. On the Estimation of a Probability Density Function and Mode. *Annals of Mathematical Statistics*, 33:1065–1076, September 1962. doi:10.1214/aoms/1177704472.

[99] Ronald L. Pease. Total-Dose Issues for Microelectronics in Space Systems. *IEEE Transactions on Nuclear Science*, 43(2):442–452, 1996.

[100] Vir V. Phoha. *The Springer Internet Security Dictionary.* Springer-Verlag, New York, 2002. doi:10.1007/b98881.

[101] John C. Platt. Probabilistic Outputs for Support Vector Machines and Comparison to Regularized Likelihood Methods. In *Advances in Large Margin Classifiers*, volume 10, pages 61–74, 2000.

[102] Eric Priest and Terry Forbes. *Magnetic Reconnection: MHD theory and applications.* Cambridge University Press, Cambridge, UK, 2000. ISBN 0-521-48179-1.

[103] QinetiQ. Satellite Payloads: Energetic Particle Telescope. Accessed January 2016. https://www.qinetiq.com/services-products/space/Pages/satellite-payloads-ept.aspx.

[104] Chotirat Ann Ratanamahatana, Jessica Lin, Dimitrios Gunopulos, Eamonn Keogh, Michail Vlachos, and Gautam Das. Mining Time Series Data. In Oded Maimon and Lior Rokach, editors, *Data Mining and Knowledge Discovery Handbook: A Complete Guide for Practitioners and Researchers*, Chapter 51, pages 1069–1103. Kluwer Academic Publishers, 2005. doi:10.1007/b107408.

[105] Geoffrey Reeves, Steve Morley, and Greg Cunningham. Long-Term Variations in Solar Wind Velocity and Radiation Belt Electrons. *Journal of Geophysical Research: Space Physics*, 118:1040–1048, March 2013. 10.1002/jgra.50126.

[106] Jaxk Reeves, Jien Chen, Xiaolan L. Wang, Robert Lund, and Qi Qi Lu. A Review and Comparison of Changepoint Detection Techniques for Climate Data. *Journal of Applied Meteorology and Climatology*, 46(6):900–915, 2007.

[107] Pete Riley. On the Probability of Occurrence of Extreme Space Weather Events. *Space Weather*, 10(2), 2012. S02012.

[108] Dennis Roddy. *Satellite Communications*, Chapter 7. McGraw-Hill, New York, Fourth edition, 2001.

[109] Stan Salvador and Philip Chan. Learning States and Rules for Time-Series Anomaly Detection. *Applied Intelligence*, 23(3):241–255, 2005. doi:10.1007/s10489-005-4610-3.

[110] Satellite Industry Association. State of the Satellite Industry. May 2015. Prepared by The Tauri Group.

[111] D. M. Sawyer and James Vette. AP-8 Trapped Proton Environment for Solar Maximum and Solar Minimum. *NASA STI/Recon Technical Report N*, 77, December 1976.

[112] Carolus Schrijver. Socio-Economic Hazards and Impacts of Space Weather: The Important Range Between Mild and Extreme. *Space Weather*, 13, 2013. doi:10.1002/2015SW001252.

[113] Nathan A. Schwadron, A. J. Boyd, K. Kozarev, M. Golightly, H. Spence, L. W. Townsend, and M. Owens. Galactic Cosmic Ray Radiation Hazard in the Unusual Extended Solar Minimum between Solar Cycles 23 and 24. *Space Weather*, 8, may 2010.

[114] James R. Schwank, Marty R. Shaneyfelt, and Paul E. Dodd. Radiation Hardness Assurance Testing of Microelectronic Devices and Integrated Circuits: Radiation Environments, Physical Mechanisms, and Foundations for Hardness Assurance. In *IEEE Transactions on Nuclear Science*, volume 60, pages 2074–2100. IEEE, June 2013.

[115] Hagit Shatkay and Stanley B. Zdonik. Approximate Queries and Representations for Large Data Sequences. In *Proceedings of the 12th International Conference on Data Engineering*, pages 536–545, March 1996. doi: 10.1109/ICDE.1996.492204.

[116] Walter Andrew Shewhart. *Economic Control of Quality of Manufactured Product.* D. Van Nostrand Company, 1931.

[117] Rasheda Smith, Alan Bivens, Mark Embrechts, Chandrika Palagiri, and Boleslaw Szymanski. Clustering Approaches for Anomaly-Based Intrusion Detection. In *Proceedings of the Intelligent Engineering Systems through Artificial Neural Networks*, pages 579–584. ASME Press, 2002.

[118] Steven W. Smith. *Digital Signal Processing: A Practical Guide for Engineers and Scientists.* Newnes, 2003. ISBN: 9780750674447.

[119] Space Studies Board. Severe Space Weather Events – Understanding Societal and Economic Impacts. *National Academy Press*, 2008.

[120] Space Systems/Loral. GOES I-M Databook. Technical Report DRL 101-08, GSFC Specification S-480-21A, Contract NAS5-29500, Reference #S-415-19, National Aeronautics and Space Administration, Goddard Space Flight Center, Greenbelt, MD, August 1996.

[121] Space Systems/Loral. Intelsat 30/DLA-1 and Intelsat 31/DLA-2, 2016. URL: http://www.sslmda.com/html/satexp/isdla1_2.html.

[122] SpaceX. About SpaceX. Accessed Nov. 22, 2015. http://www.spacex.com/about.

[123] Harlan E. Spence, A.W. Case, M.J. Golightly, T. Heine, B.A. Larsen, J.B. Blake, P. Caranza, W.R. Crain, J. George, M. Lalic, A. Lin, M.D. Looper, J.E. Mazur, D. Salvaggio, J.C. Kasper, T.J. Stubbs, M. Doucette, P. Ford, R. Foster, R. Goeke, D. Gordon, B. Klatt, J. O'Connor, M. Smith, T. Onsager, C. Zeitlin, L.W. Townsend, and Y. Charara. CRaTER: The Cosmic Ray Telescope for the Effects of Radiation Experiment on the Lunar Reconnaissance Orbiter Mission. *Space Science Reviews: Astronomy, Astrophysics & Space Science*, 150:243–284, 2010.

[124] Joseph Srour and James McGarrity. Radiation Effects on Microelectronics in Space. In *Proceedings of the IEEE*, volume 76, pages 1443–1469, November 1988. doi:10.1109/5.90114.

[125] Pei Sun, Sanjay Chawla, and Bavani Arunasalam. Mining for Outliers in Sequential Databases. In *SIAM International Conference on Data Mining*, Bethesda, MD, 2006. Society for Industrial and Applied Mathematics. doi:10.1137/1.9781611972764.9.

[126] Pang-Ning Tan, Michael Steinbach, and Vipin Kumar. *Introduction to Data Mining.* Pearson Addison-Wesley, Boston, June 2006.

[127] The Tauri Group. Start-Up Space: Rising Investment in Commercial Space Ventures. January 2016.

[128] Teledyne Microelectronic Technologies. Micro Dosimeter Datasheet. Accessed August 2015. http://www.teledynemicro.com/_documents/Datasheets/UDOS001_Micro_Dosimeter_Datasheet.pdf.

[129] Massimo Tipaldi and Bernhard Bruenjes. Spacecraft Health Monitoring and Management Systems. In *IEEE Metrology for Aerospace*, pages 68–72, Benevento, Italy, May 2014. doi: 10.1109/MetroAeroSpace.2014.6865896.

[130] Gabor Toth, Igor V. Sokolov, Tamas I. Gombosi, David R. Chesney, C. Robert Clauer, Darren L. De Zeeuw, Kenneth C. Hansen, Kevin J. Kane, Ward B. Manchester, Robert C. Oehmke, Kenneth G. Powell, Aaron J. Ridley, Ilia I. Roussev, Quentin F. Stout, Ovsei Volberg, Richard A. Wolf, Stanislav Sazykin, Anthony Chan, Bin Yu, and Jozsef Kota. Space Weather Modeling Framework: A New Tool for the Space Science Community. *Journal of Geophysical Research: Space Physics*, 110(A12), 2005. A12226.

[131] Ernie Tretkoff. Space Weather and Satellite Engineering: An Interview With Michael Bodeau. *Space Weather*, 8(3), 2010. S03003.

[132] Bruce Tsurutani, Christian Ho, John Arballo, Bruce Goldstein, and Andre Balogh. Large Amplitude IMF Fluctuations in Corotating Interaction Regions: Ulysses at Midlatitudes. *Geophysical Research Letters*, 22(23):397–3400, December 1995. doi:10.1029/95GL03179.

[133] John W. Tukey. *Exploratory Data Analysis.* Pearson, 1977. ISBN: 978-0201076165.

[134] James Vette. The AE-8 Trapped Electron Model Environment. *NASA STI/Recon Technical Report N*, 92, November 1991.

[135] Wall Street Journal. AT&T Declares Its Satellite Permanently Out of Service. http://www.wsj.com/articles/SB85351142012308000, January 1997.

[136] A. Wander and R. Forstner. Innovative Fault Detection Isolation and Recovery Strategies On-Board Spacecraft: State of the Art and Research Challenges. In *Deutscher Luft- und Raumfahrtkongress*, Berlin, 2012.

[137] Chengwei Wang, Lakshminarayan Choudur Krishnamurthy Viswanathan, Vanish Talwar, Wade Satterfield, and Karsten Schwan. Statistical Techniques for Online Anomaly Detection in Data Centers. In *IEEE International Symposium on Integrated Network Management*, May 2011.

[138] Yao Wang, Chunguo Wu, Zhaohua Ji, Binghong Wang, and Yanchun Liang. Non-Parametric Change-Point Method for Differential Gene Expression Detection. *PLoS ONE*, 6(5), May 2011. doi:10.1371/journal.pone.0020060.

[139] Christina Warrender, Stephanie Forrest, and Barak Pearlmutter. Detecting Intrusions using System Calls: Alternate Data Models. In *IEEE Symposium on Security and Privacy*, pages 133–145, Oakland, CA, 1999. IEEE. doi:10.1109/SECPRI.1999.766910.

[140] Andreas S. Weigend, Morgan Mangeas, and Ashok N. Srivastava. Nonlinear Gated Experts for Time-Series: Discovering Regimes and Avoiding Overfitting. *International Journal of Neural Systems*, 6(4):373–399, 1995.

[141] James R. Wertz and Wiley J. Larson. *Space Mission Engineering: The New SMAD.* Microcosm, Portland, OR, third edition, October 1999.

[142] Franklin E. White. Data Fusion Lexicon. Technical report, Data Fusion Panel, Joint Directors of Laboratories, Technical Panel for C3, 1987.

[143] Daniel Wilkinson, Stuart Daughtridge, John Stone, Herbert Sauer, and Phil Darling. TDRS-1 Single Event Upsets and the Effect of the Space Environment. In *IEEE Transactions on Nuclear ScienceE*, volume 38, pages 1708–1712. IEEE, December 1991. doi:10.1109/23.124166.

[144] J. Rudolph Wolf. Nachrichten von der Sternwarte in Berne. In *Mittheilungen der Naturforschenden Gesellschaft in Bern*, pages 169–173, 1848.

[145] Wilson W. S. Wong and James Fergusson. *Military Space Power: A Guide to the Issues.* Contemporary Military, Strategic, and Security Issues. Praeger, Santa Barbara, CA, 2010.

[146] World Data Center, Data Analysis Center for Geomagnetism and Space Magnetism. Geomagnetic Equatorial Dst Index Home Page. Accessed: August 2015. URL: http://wdc.kugi.kyotou.ac.jp/dstdir/index.html.

[147] World Data Center, Royal Observatory of Belgium, avenue Circulaire 3, 1180 Brussels, Belgium. Sunspot Index and Long-term Solar Observations (SISLO), 1991–2015. International Sunspot Number Monthly Bulletin and online catalogue. Accessed: August 2015. URL: http://www.sidc.be/silso/.

[148] Gordon Wrenn. Conclusive Evidence for Internal Dielectric Charging Anomalies on Geosynchronous Communications Spacecraft. *Journal of Spacecraft and Rockets*, 32(3):514–520, May 1995. doi:10.2514/3.26645.

[149] Kenji Yamanishi, Jun ichi Takeuchi, Graham Williams, and Peter Milne. Online Unsupervised Outlier Detection Using Finite Mixtures with Discounting Learning Algorithms. In *Proceedings of the Sixth ACM SIGKDD International Conference on Knowledge Discovery and Data Mining*, pages 320–324, Boston, MA, August 2000.